


# The RNA exosome complex degrades expanded hexanucleotide repeat RNA in *C9orf72* FTLD/ALS

Yuya Kawabe , Kohji Mori\* , Tomoko Yamashita, Shiho Gotoh  & Manabu Ikeda

## Abstract

Nucleotide repeat expansions in the *C9orf72* gene cause frontotemporal lobar degeneration (FTLD) and amyotrophic lateral sclerosis (ALS). Transcribed repeat RNA accumulates within RNA foci and is also translated into toxic dipeptide repeat proteins (DPR). The mechanism of repeat RNA accumulation, however, remains unclear. The RNA exosome complex is a multimeric ribonuclease involved in degradation of defective RNA. Here, we uncover the RNA exosome as a major degradation complex for pathogenic *C9orf72*-derived repeat RNA. Knockdown of EXOSC10, the catalytic subunit of the complex, enhanced repeat RNA and DPR protein expression levels. RNA degradation assays confirmed that EXOSC10 can degrade both sense and antisense repeats. Furthermore, EXOSC10 reduction increased RNA foci and repeat transcripts in patient-derived cells. Cells expressing toxic poly-GR or poly-PR proteins accumulate a subset of small nucleolar RNA precursors, which are physiological substrates of EXOSC10, as well as excessive repeat RNA, indicating that arginine-rich DPR proteins impair the intrinsic activity of EXOSC10. Collectively, arginine-rich DPR-mediated impairment of EXOSC10 and the RNA exosome complex compromises repeat RNA metabolism and may thus exacerbate *C9orf72*-FTLD/ALS pathologies in a vicious cycle.

**Keywords** dipeptide repeat proteins; DIS3; EXOSC10; RAN translation; RNA metabolism in neurodegeneration

**Subject Categories** Neuroscience; RNA Biology

**DOI** 10.15252/emboj.2019102700 | Received 16 June 2020 | Revised 19 July 2020 | Accepted 23 July 2020 | Published online 24 August 2020

**The EMBO Journal (2020) 39: e102700**

## Introduction

Frontotemporal lobar degeneration (FTLD) and amyotrophic lateral sclerosis (ALS) are currently incurable neurodegenerative disorders with distinct but overlapping phenotypes. The hexanucleotide repeat expansion in *C9orf72* gene is the most common known genetic cause of FTLD/ALS (DeJesus-Hernandez *et al.*, 2011; Renton *et al.*, 2011; Gijselinck *et al.*, 2012). The hexanucleotide DNA repeat is bidirectionally transcribed into GGGGCC ( $G_4C_2$ ) or CCCC GG

( $C_4G_2$ ) repeat RNAs. The repeat RNA accumulates and forms RNA foci that sequester selective repeat RNA binding protein (RBP)s and thereby physiological function of the RBPs might be impaired. The  $G_4C_2$  and  $C_4G_2$  RNA repeats are even translated into five distinct dipeptide repeat protein (DPR) in the absence of AUG initiation codon through repeat-associated non-AUG dependent (RAN) translation (Ash *et al.*, 2013; Gendron *et al.*, 2013; Mori *et al.*, 2013a,c; Zu *et al.*, 2013). DPR toxicity has been extensively studied and validated in multiple disease models (May *et al.*, 2014; Mizielińska *et al.*, 2014; Zhang *et al.*, 2016, 2018b). *C9orf72* protein coded in the exons of *C9orf72* has been functionally linked to vesicular trafficking and autophagy (Farg *et al.*, 2014; Sellier *et al.*, 2016; Webster *et al.*, 2016; Yang *et al.*, 2016; Aoki *et al.*, 2017). *C9orf72* haploinsufficiency exacerbated repeat-dependent toxicity suggesting loss of *C9orf72* function may also contribute to neurodegeneration in *C9orf72* FTLD/ALS (Shi *et al.*, 2018; Boivin *et al.*, 2020; Zhu *et al.*, 2020). Since the expansion hinder efficient transcription, mature *C9orf72* mRNA transcript levels are consistently decreased in *C9orf72* cases (DeJesus-Hernandez *et al.*, 2011; van Blitterswijk *et al.*, 2015). In clear contrast, the RNA expression levels of the repeat flanking region are much increased in *C9orf72* patients compared to that of the controls (Mori *et al.*, 2013c). These contradicting findings imply that the repeat RNA accumulates despite inefficient transcription. As an explanation for this discrepancy, we hypothesized the *C9orf72* repeat RNA might resist to efficient RNA degradation in *C9orf72* FTLD/ALS.

The multiprotein complex RNA exosome (Fig EV1A) is involved in RNA quality control through degradation of defective RNAs. The RNA exosome can equip two different active centers for RNA degradation at the top [EXOSC10 (Rrp6 in yeast)] and bottom [DIS3 (Rrp44 in yeast) or DIS3L] of the complex (Kilchert *et al.*, 2016). Combinations of catalytic components of the RNA exosome complex are different depending on its subcellular localization (Tomecki *et al.*, 2010). EXOSC10 and DIS3 contain nuclear localization signals (Graham *et al.*, 2009) and physiologically distribute in the nucleus. Within the nucleus, EXOSC10, but not DIS3, is strongly enriched in the nucleoli (Tomecki *et al.*, 2010). Moreover, a DIS3 homologue DIS3L is largely restricted to the cytoplasm possibly due to its lack of nuclear localization signal (Tomecki *et al.*, 2010).

Several components of the RNA exosome complex are already linked to neurodegenerative phenotypes. Homozygous or compound heterozygous genetic mutations in either EXOSC3, EXOSC8, or

EXOSC9 has been linked to autosomal recessive developmental pontocerebellar hypoplasia, type1b (OMIM #614678) (Wan *et al*, 2012), type1c (OMIM #616081) (Boczonadi *et al*, 2014), or type1d (OMIM #618065) (Burns *et al*, 2018) presenting diffuse muscle weakness and progressive microcephaly. These evidences suggest proper RNA processing through the RNA exosome complex is indispensable for the development and survival of neurons. By using cellular models of *C9orf72* FTL/ALS, here we reveal that the RNA exosome complex, especially its catalytic component EXOSC10, is involved in degradation of the *C9orf72* repeat RNA. This is further confirmed in RNA degradation assay and in patient-derived cells. Expanded repeat RNA and/or DPRs have been reported to induce nucleocytoplasmic transport impairment and nucleolar stress (Freibaum *et al*, 2015; Zhang *et al*, 2015, 2018a; Mizielinska *et al*, 2017). We find frequent mislocalization of EXOSC10 in cells expressing arginine-rich DPR in RAN translation-dependent manner. Moreover, co-immunoprecipitation assay reveals arginine-rich DPR binds with EXOSC10. With these DPR, functional impairment of EXOSC10 is evident from the accumulation of its endogenous substrate, 3'extended small nucleolar RNA (snoRNA) precursors (Allmang *et al*, 1999a; Davidson *et al*, 2019). Strikingly, cells expressing arginine-rich DPR show increased accumulation of co-expressed repeat RNA. These results suggest arginine-rich DPR causes functional impairment of the RNA exosome complex which leads to accumulation of repeat RNA and thus further deposition of RNA foci and DPR.

## Results

### The RNA exosome component EXOSC10 regulates *C9orf72* G<sub>4</sub>C<sub>2</sub> repeat RNA metabolism in a cellular model of *C9orf72* repeat expansion

To examine potential contribution of the RNA exosome complex (Fig EV1A) on *C9orf72* repeat RNA degradation, we applied previously developed repeat-transfected cellular model that express both RNA foci and DPR from (G<sub>4</sub>C<sub>2</sub>)<sub>80</sub> repeats (Mori *et al*, 2013c, 2016; Fig 1A). The reporter (G<sub>4</sub>C<sub>2</sub>)<sub>80</sub> repeat construct has endogenous 113 bp 5'UTR region of the G<sub>4</sub>C<sub>2</sub> repeat. This 113 bp 5'UTR region does not contain any ATG start codon but contain multiple stop

codons in all three possible reading frames. Therefore, the translation of DPR only driven in a RAN translation-dependent manner (Fig 1A). Knockdown of EXOSC10 but not of DIS3 and DIS3L significantly augmented generation of DPR (poly-glycine-alanine (GA)) in HeLa cells expressing (G<sub>4</sub>C<sub>2</sub>)<sub>80</sub> repeats under the EF1 promoter (Figs 1B and C, and EV1B and C). RT-qPCR analysis confirmed a corresponding increase of G<sub>4</sub>C<sub>2</sub> repeat RNA upon EXOSC10 knockdown (Fig 1D). Consistent with RT-qPCR analysis, EXOSC10 knockdown visualized more G<sub>4</sub>C<sub>2</sub> repeat RNA foci (Figs 1E and F, and EV1D). Cellular RNA foci intensity was also increased upon EXOSC10 knockdown (Fig 1G). Conversely, ectopic expressions of increasing doses of siRNA-resistant EXOSC10 rescued poly-GA generation in a dose-dependent manner upon knockdown of endogenous EXOSC10 (Fig 2A and B). Complementary expression of EXOSC10 also rescued repeat RNA expression (Fig 2C). Moreover, simple overexpression of EXOSC10 also suppressed repeat RNA expression in the absence of prior EXOSC10 knockdown (Fig 2D). Together, these results suggest that EXOSC10 is a significant determinant for repeat RNA metabolism and thus for DPR expression in our cellular model of *C9orf72* repeat expansion.

### EXOSC10 degrades *C9orf72* hexanucleotide repeat RNA in *in vivo* and *in vitro* RNA degradation assays

To confirm EXOSC10 indeed affect repeat RNA stability in cells, we performed *in vivo* RNA stability assay by treating repeat-transfected HeLa cells with actinomycin D (a classic transcription inhibitor) to inhibit *de novo* transcription of repeat RNA. As expected, cells with EXOSC10 knockdown showed more stable expression of the G<sub>4</sub>C<sub>2</sub> repeat RNA during experimental time course when compared to cells with non-targeting siRNA knockdown (Fig 3A). This result suggests that EXOSC10 indeed regulates G<sub>4</sub>C<sub>2</sub> repeat RNA metabolism in cells. Moreover, a similar effect was observed when 30 repeats of antisense CCCC GG repeat (C<sub>4</sub>G<sub>2</sub>)<sub>30</sub> was used instead of (G<sub>4</sub>C<sub>2</sub>)<sub>80</sub> (Fig 3B). This suggests EXOSC10 is also involved in the metabolism of antisense C<sub>4</sub>G<sub>2</sub> repeat RNA in cells.

To examine more direct effect of EXOSC10 on G<sub>4</sub>C<sub>2</sub> and C<sub>4</sub>G<sub>2</sub> repeat RNA degradation, *in vitro* RNA degradation assay was performed. N-terminally GST-tagged recombinant human EXOSC10 was mixed with synthetic 5'FAM-labeled (G<sub>4</sub>C<sub>2</sub>)<sub>8</sub> repeat RNA or (C<sub>4</sub>G<sub>2</sub>)<sub>8</sub> repeat RNA. Since EXOSC10 is a 3'exoribonuclease, 3' PO<sub>4</sub><sup>3-</sup>-

#### Figure 1. Knockdown of EXOSC10 increases repeat RNA and poly-GA expression.

- A Schematic representation of a plasmid expressing (G<sub>4</sub>C<sub>2</sub>)<sub>80</sub> repeats together with 5' flanking of the *C9orf72* repeat (113 bp) and artificially introduced 3' 3xTAG.
- B, C siRNA-mediated knockdown of EXOSC10 (EXO10), but not of DIS3 and DIS3L, significantly increased generation of poly-GA in HeLa cells expressing (G<sub>4</sub>C<sub>2</sub>)<sub>80</sub> repeats. 3 independent experiments. Each experiment performed in duplicates. "ctrl" indicates a control vector which lacks the G<sub>4</sub>C<sub>2</sub> repeat but still contains the 5' flanking region and 3xTAG.
- D Increased G<sub>4</sub>C<sub>2</sub> repeat RNA expression upon EXOSC10 knockdown on RT-qPCR. 4 independent experiments. Each experiment performed in duplicates.
- E, F Knockdown of EXOSC10 increased RNA foci in HeLa cells expressing (G<sub>4</sub>C<sub>2</sub>)<sub>80</sub> repeats visualized by *in situ* hybridization targeting sense RNA foci. In total, 25 (Ct) and 24 (EXO10<sub>#5</sub>) images were analyzed in 3 independent experiments. Scale bar = 10 μm.
- G Knockdown of EXOSC10 increased RNA foci intensity in HeLa cells expressing (G<sub>4</sub>C<sub>2</sub>)<sub>80</sub> repeats. Each dot represents average cellular RNA foci intensity (Arbitrary unit) of RNA foci-positive cells in each randomly taken image. In total, 25 (Ct) and 24 (EXO10<sub>#5</sub>) images were analyzed in 3 independent experiments.

Data information: All graphs except (G) are shown as mean ± SEM. (G) is shown in box-and-whisker plot (the central band is the median the ends of the box represent the 1<sup>st</sup> and 3<sup>rd</sup> quartile, the whiskers extend from the ends of the box to the outermost data point that falls within "3<sup>rd</sup> quartile + 1.5 × interquartile range" to "1<sup>st</sup> quartile - 1.5 × interquartile range"). \*P < 0.05, \*\*\*P < 0.001; ANOVA with Dunnett's post-test vs. Ct (=control) (C) or two-tailed unpaired t-test (D, F, G). A dot in graph represents a data point from single well of cell culture plate (C, D, F). Ct: non-targeting siRNA. EXO10<sub>#5</sub>: a siRNA targeting EXOSC10.

Source data are available online for this figure.

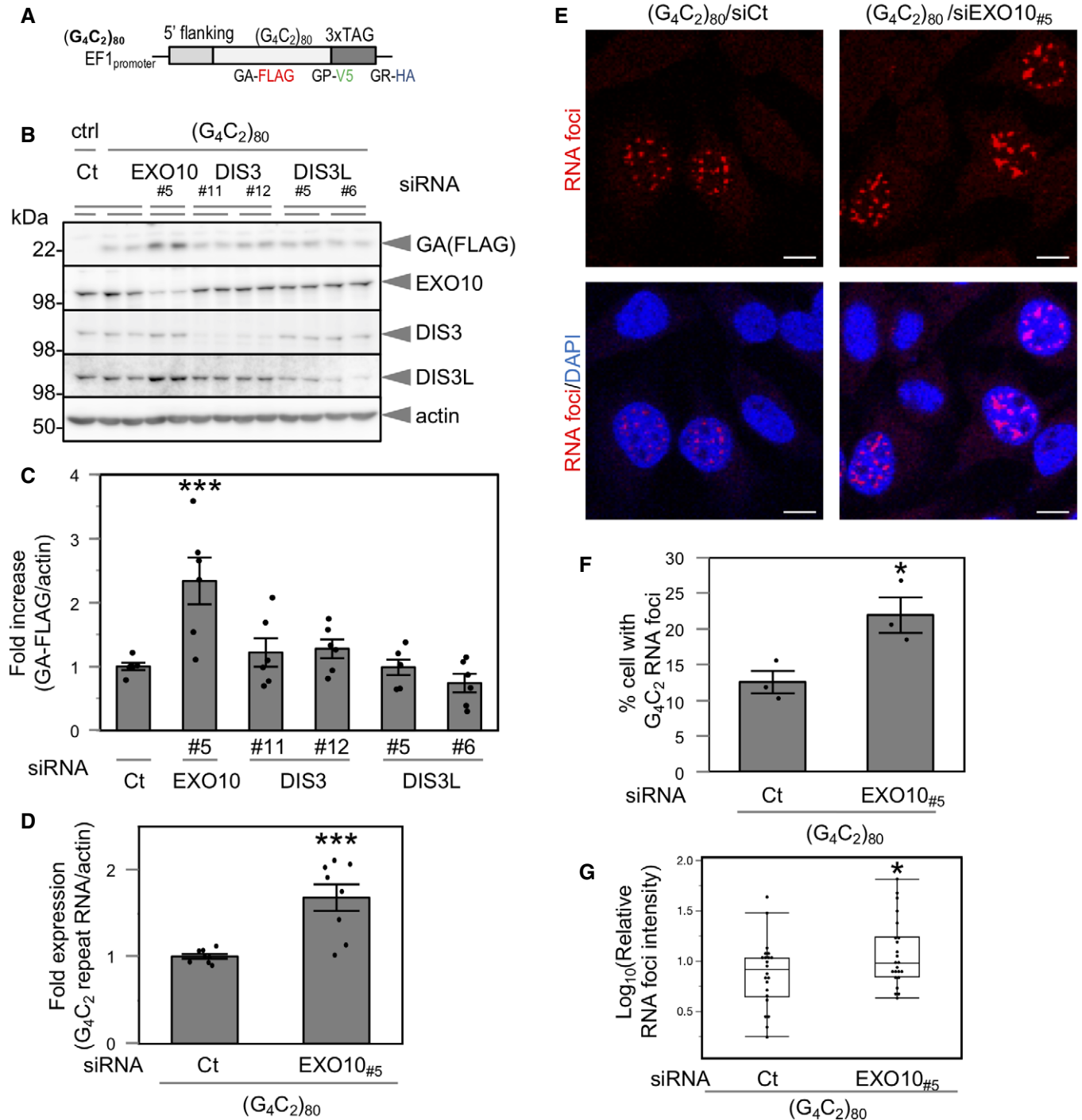
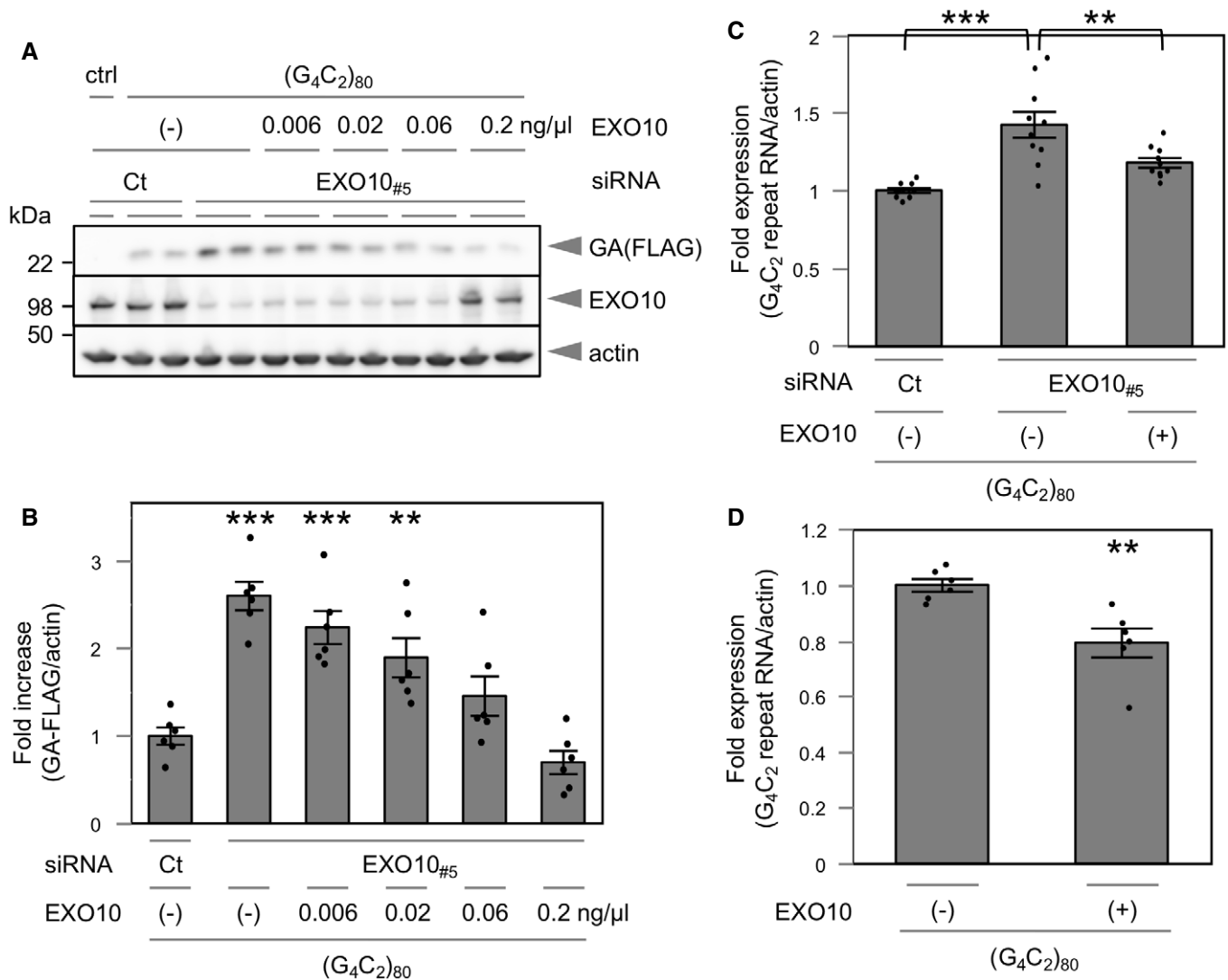


Figure 1.

labeled  $(G_4C_2)_8$  repeat RNA is also tested as negative control (blocked substrate). The mixtures containing one of each substrate were then incubated in the presence of recombinant RNase inhibitor (to prevent unintentional RNA degradation through potentially contaminating RNase A, B, and C) and analyzed with TBE-Urea gel electrophoresis (Fig 3C–F). Recombinant EXOSC10 shows time-dependent degradation of synthetic  $G_4C_2$  repeat RNA, while 3'  $PO_4^{3-}$ -labeled blocked  $G_4C_2$  repeat RNA is not degraded at all. Lack

of recombinant EXOSC10 or  $Mg^{2+}$  ion (essential co-factor for EXOSC10 activity) abolished the RNA degradation activity, further validating EXOSC10-mediated  $G_4C_2$  repeat degrading activity (Fig 3C and D). Moreover, recombinant EXOSC10 also shows time-dependent degradation of antisense  $C_4G_2$  repeat RNA (Fig 3E and F). These *in vivo* and *in vitro* results provide further evidence that EXOSC10 contributes to the degradation of *C9orf72* sense and antisense repeat RNA.



**Figure 2. Suppression of repeat RNA and poly-GA by EXOSC10 expression.**

A, B Dose-dependent suppression of poly-GA by exogenous EXOSC10 upon EXOSC10 knockdown. 3 independent experiments. Each experiment performed in duplicates.

C Suppression of G<sub>4</sub>C<sub>2</sub> repeat RNA by exogenous EXOSC10 on EXOSC10 knockdown. 5 independent experiments. Each experiment performed in duplicates. Concentration of transfected EXOSC10 plasmid was 0.2 ng/μl in 1 ml medium.

D Overexpression of EXOSC10 decreases G<sub>4</sub>C<sub>2</sub> repeat RNA. 3 independent experiments.

Data information: All graphs are shown as mean ± SEM. \*\**P* < 0.01, \*\*\**P* < 0.001; ANOVA with Dunnett's post-test vs. Ct (B) or with Turkey-Kramer's post-test (C), two-tailed unpaired *t*-test (D). A dot in graph represents a data point from single well of cell culture plate. Ct: non-targeting siRNA. EXO10<sub>#5</sub>: an siRNA targeting EXOSC10. Source data are available online for this figure.

### EXOSC10 reduction increases the RNA foci and repeat transcripts in fibroblasts from *C9orf72* repeat expansion carriers

Repeat RNA expressed from plasmid-based reporter contains artificial sequence from linker region, TAG region, and plasmid backbone. Next, we asked whether EXOSC10 degrades the endogenous sense and antisense repeat RNA in human primary cells. To do so, EXOSC10 knockdown was performed on fibroblasts from three *C9orf72* patients (Mori *et al*, 2016; Zhou *et al*, 2017). The demographics of these patients were previously described (Mori *et al*, 2016; Zhou *et al*, 2017) and summarized in Appendix Fig S1A. The

sense and antisense RNA foci could be visualized through *in situ* hybridization in *C9orf72* fibroblasts (Figs 4A and EV2A) as previously described (Donnelly *et al*, 2013; Mori *et al*, 2016). Western blot analysis confirmed efficient suppression of EXOSC10 upon siRNA-mediated knockdown (Fig EV2B and C). Upon EXOSC10 knockdown, % cells with G<sub>4</sub>C<sub>2</sub> repeat RNA foci and number of G<sub>4</sub>C<sub>2</sub> repeat RNA foci per cell increased (Fig 4B and C, Appendix Fig S1B). Similarly, % cells with antisense C<sub>4</sub>G<sub>2</sub> repeat RNA foci and the number of C<sub>4</sub>G<sub>2</sub> repeat RNA foci per cell increased with EXOSC10 knockdown (Fig 4D and E, Appendix Fig S1B). Consistent with *in situ* hybridization analysis, strand-specific RT-qPCR analysis

targeting 3' flanking region of endogenous G<sub>4</sub>C<sub>2</sub> repeat (=5' flanking region of C<sub>4</sub>G<sub>2</sub> repeat) revealed increased endogenous sense and antisense repeat RNA expression upon EXOSC10 knockdown (Fig 4F and G). These results suggest that EXOSC10 contributes the metabolism of disease-associated sense and antisense repeat RNA with endogenous sequence contexts in *C9orf72* patient-derived cells.

**DIS3 compensates G<sub>4</sub>C<sub>2</sub> repeat RNA degradation in the absence of EXOSC10**

EXOSC10 plays two major roles in RNA degradation. One is direct substrate degradation via its intrinsic exoribonuclease activity through the DEDDy and HRDC domains (Januszzyk et al, 2011). The

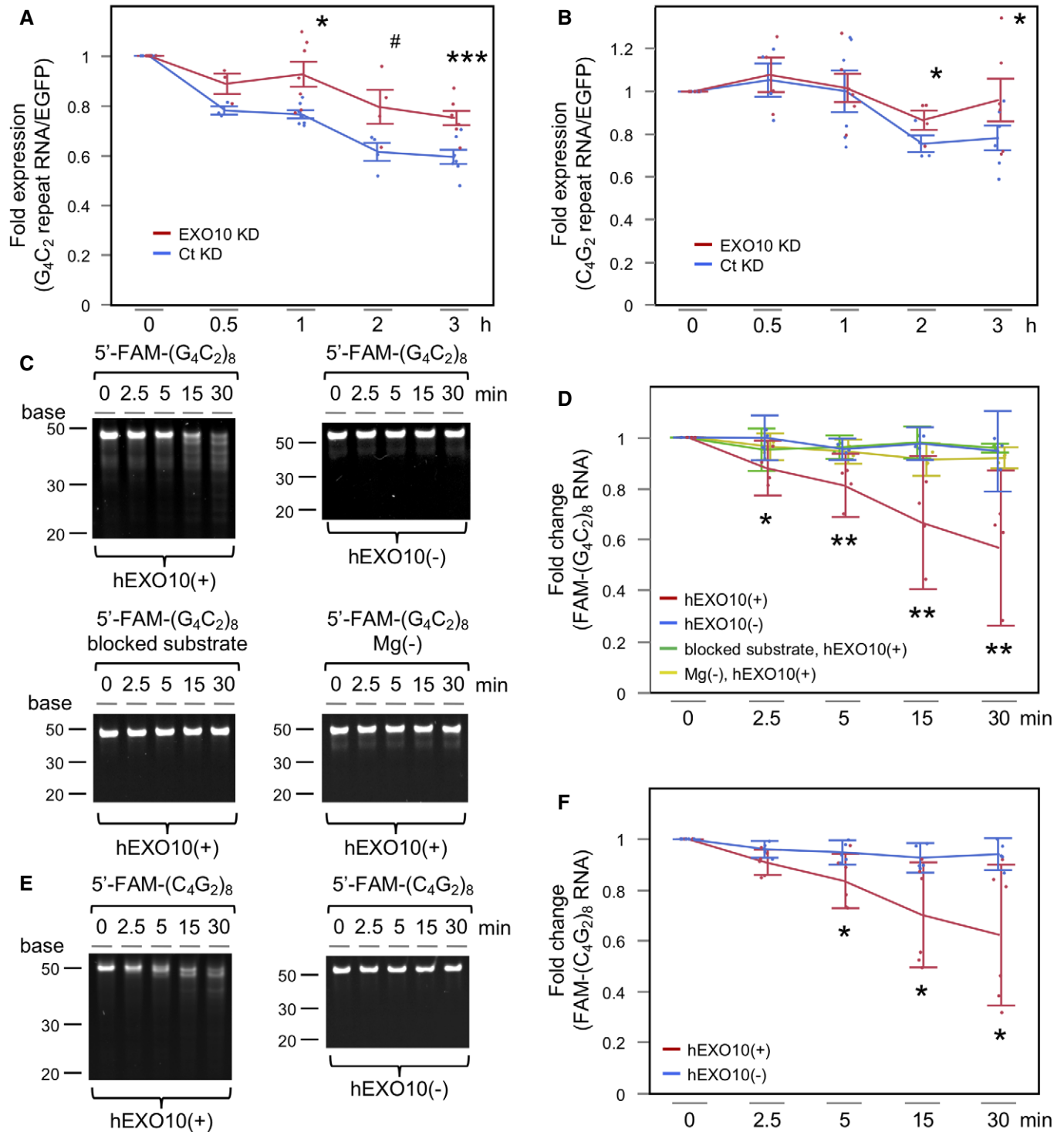


Figure 3.

**Figure 3. EXOSC10 degrades hexanucleotide repeat RNA *in vivo* and *in vitro*.**

- A, B Under transcription inhibition with actinomycin D, cells with EXOSC10 knockdown (EXO10 KD) showed more stable expression of the repeat RNA compared to cells with control knockdown with non-targeting siRNA (Ct KD). 7 and 6 independent experiments were performed.
- C, D Degradation of FAM-labeled synthetic (G<sub>4</sub>C<sub>2</sub>)<sub>8</sub> repeat RNA with recombinant human EXOSC10 (hEXO10) (Upper left). 3' blocked FAM-labeled G<sub>4</sub>C<sub>2</sub> repeat RNA resisting 3' exoribonuclease activity is not degraded by recombinant EXOSC10 (Lower left). Lack of recombinant EXOSC10 (Upper right) or Mg<sup>2+</sup> ion which is essential co-factor of EXOSC10 (Lower right) abolished the RNA degradation activity. 3 or 4 independent experiments. Quantification of the top bands is shown in (D).
- E, F Degradation of antisense C<sub>4</sub>G<sub>2</sub> repeat RNA substrate with recombinant human EXOSC10 (Left). Without recombinant EXOSC10, no substrate degradation was observed (Right). 5 or 6 independent experiments. Quantification is shown in (F).

Data information: Graph (A, B) are shown as mean ± SEM. Graph (D, F) are shown as mean ± 95% CI. #*P* = 0.1144, \**P* < 0.05, \*\**P* < 0.01, \*\*\**P* < 0.001; two-tailed paired *t*-test at each time point (A, B), ANOVA with Dunnett's post-test vs. hEXO10(−) at each time point (D) or two-tailed unpaired *t*-test at each time point (F). A dot in graph (A, B) represents a data point from single well of cell culture plate. A dot in graph (D, F) represents a data obtained from an aliquot of a reaction mixture sequentially obtained at each time point (0, 2.5, 5, 15, 30 min).

other is efficient guidance of substrate RNA into the central tunnel of barrel-like structure which is formed by catalytically inert nine core subunits called Exo1-9 and thus facilitate DIS3-dependent substrate RNA degradation (Fig EV1A; Kilchert *et al*, 2016; Wasmuth & Lima, 2017).

Once passed through the barrel-like structure, RNA substrate is expected to be degraded by DIS3 (Bonneau *et al*, 2009; Malet *et al*, 2010; Drazkowska *et al*, 2013; Makino *et al*, 2013; Wasmuth *et al*, 2014). While DIS3 knockdown alone did not show clear effect on poly-GA expression (Fig 1B and C), we wondered DIS3 activity might be hidden behind the excessive activity of EXOSC10. To test the notion, we performed additive knockdown of DIS3 on top of EXOSC10 knockdown. As expected, double knockdown of EXOSC10 and DIS3 resulted in a significant increase in poly-GA expression compared to single EXOSC10 knockdown (Fig 5A and B). This was further confirmed at RNA expression level (Fig 5C). Furthermore, overexpression of DIS3 suppressed EXOSC10 knockdown-induced G<sub>4</sub>C<sub>2</sub> repeat RNA accumulation (Fig 5D). These results suggest that DIS3 can compensate G<sub>4</sub>C<sub>2</sub> repeat RNA degradation in the absence of EXOSC10, while EXOSC10 plays primary role in the RNA exosome complex dependent C9orf72 repeat RNA degradation. To further characterize EXOSC10's mechanism of action, we generated catalytically dead version of EXOSC10 (containing D313N + E315Q + D371N triple mutations on its catalytic center) (Januszyk *et al*, 2011). Although 3' exoribonuclease activity is lost

with these mutations, catalytically dead EXOSC10 still be able to promote DIS3-mediated RNA degradation in yeast model possibly through facilitating substrate access of the exosome complex (Wasmuth & Lima, 2012).

We then compared rescue activity of wild-type and catalytically dead EXOSC10 on (G<sub>4</sub>C<sub>2</sub>)<sub>80</sub> repeats expressing cells under EXOSC10 knockdown. In this condition, we found the catalytically dead EXOSC10 still be able to rescue the EXOSC10 knockdown-induced GA increase to a similar degree with wild-type EXOSC10 (Fig 5E and F). This result provides further support for dual actions of EXOSC10 on repeat RNA degradation, i.e., RNase activity of its own (directly shown through *in vitro* RNA degradation assay) and promotion of substrate access through the RNA exosome complex which facilitates DIS3-mediated RNA degradation (Wasmuth & Lima, 2012).

#### Arginine-rich DPR expressed from hexanucleotide repeat expansion contributes dysregulated extranucleolar distribution of EXOSC10

The five DPR species have very distinct biophysical properties. Poly-GA DPR is the most abundant, highly hydrophobic and aggregation-prone DPR (Mackenzie *et al*, 2013; Mori *et al*, 2013c). Arginine (R)-rich DPRs namely poly-glycine-arginine (GR) and poly-proline-arginine (PR) accumulate within the RNA granules and nucleoli in cellular models (Kwon *et al*, 2014; Wen *et al*, 2014; Lee *et al*, 2016).

**Figure 4. Knockdown of EXOSC10 increases RNA foci and repeat RNA transcripts in cells derived from C9orf72 mutation carriers.**

- A *In situ* hybridization. G<sub>4</sub>C<sub>2</sub> RNA foci were detected in a C9 patient-derived fibroblast but not in a control-derived fibroblast with non-targeting siRNA treatment (left panels, control/si Ct; middle panels, C9/si Ct). Knockdown of EXOSC10 increased RNA foci (right panels, C9/siEXO10<sub>#5</sub>). Nuclei were stained with DAPI (blue). White arrows indicate nuclear RNA foci. The green arrows show cytoplasmic RNA foci. Scale bar = 10 μm.
- B Quantification of %cell with G<sub>4</sub>C<sub>2</sub> RNA foci. 3 independent knockdown experiments were performed. 10 DAPI-positive cells per experiment were randomly selected, and z-stack images were obtained. In total, z-stack images from 90 cells per group (control siRNA or EXOSC10 siRNA) were counted for RNA foci.
- C Quantification of the number of G<sub>4</sub>C<sub>2</sub> RNA foci/cell. 3 independent knockdown experiments were performed. 10 DAPI-positive cells per experiment were randomly selected, and z-stack images were obtained. In total, z-stack images from 90 cells per group (control siRNA or EXOSC10 siRNA) were counted for RNA foci.
- D Quantification of %cell with C<sub>4</sub>G<sub>2</sub> RNA foci. 3 independent knockdown experiments were performed. 10 DAPI-positive cells per experiment were randomly selected, and z-stack images were obtained. In total, z-stack images from 90 cells per group (control siRNA or EXOSC10 siRNA) were counted for RNA foci.
- E Quantification of the number of C<sub>4</sub>G<sub>2</sub> RNA foci/cell. 3 independent knockdown experiments were performed. 10 DAPI-positive cells per experiment were randomly selected, and z-stack images were obtained. In total, z-stack images from 90 cells per group (control siRNA or EXOSC10 siRNA) were counted for RNA foci.
- F, G Increased endogenous repeat RNA expression upon EXOSC10 knockdown in strand-specific RT-qPCR. Ten independent knockdown experiments (Case 1 *N* = 4, Case 2 *N* = 4, Case 3 *N* = 2) were performed.

Data information: Graph (B–E) are shown as mean ± 95% CI. Graph (F, G) are shown as mean ± SEM. \**P* < 0.05, \*\**P* < 0.01, \*\*\**P* < 0.001; two-tailed unpaired *t*-test (B–G). Single dot in graph (B–E) represents an average value from 10 different cells from a coverslip. A dot in graph (F, G) represents a data point from single well of cell culture plate. Ct: non-targeting siRNA. EXO10<sub>#5</sub>: an siRNA targeting EXOSC10. Additional information is summarized in Appendix Fig S1. Source data are available online for this figure.

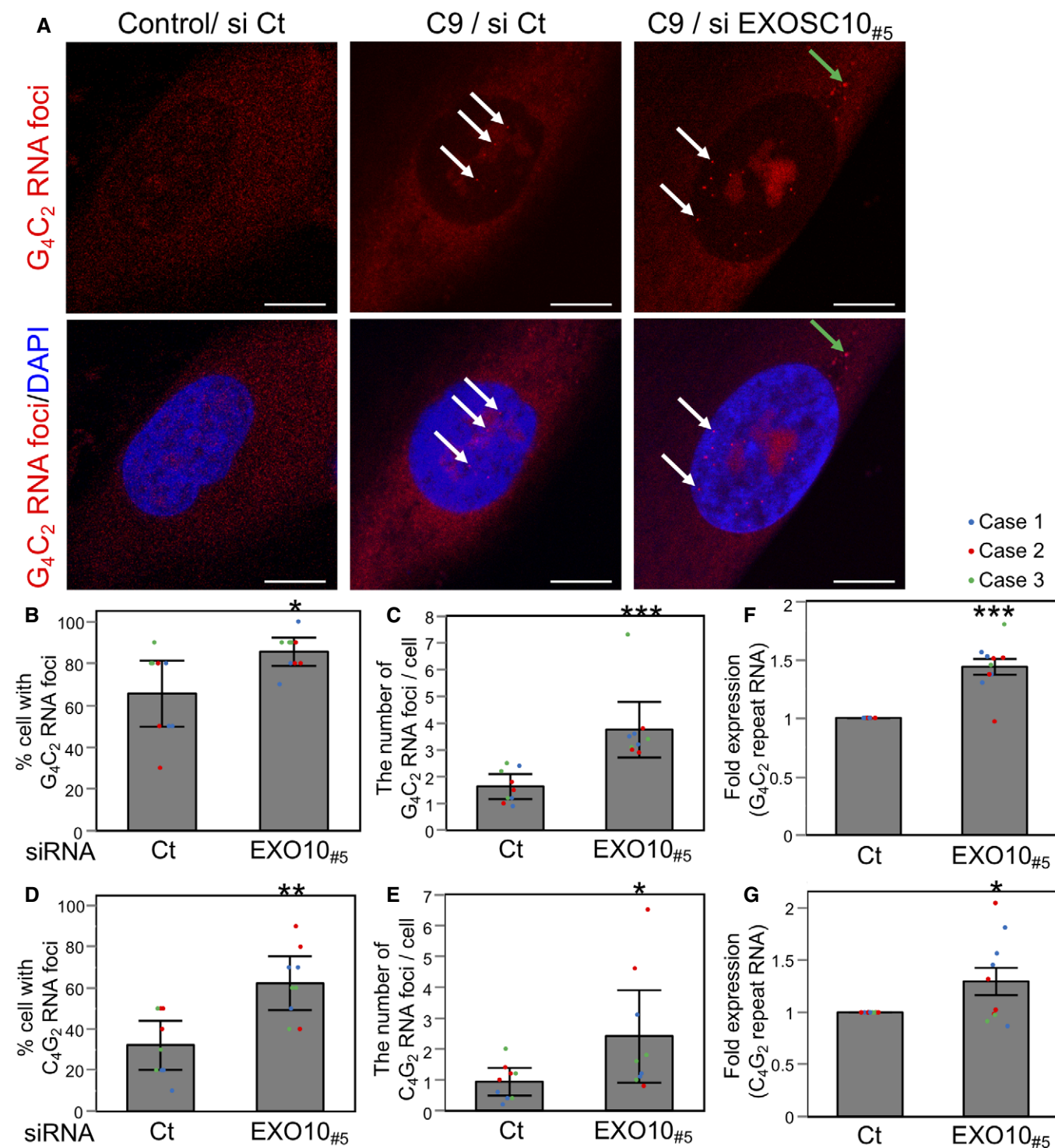


Figure 4.

Since the expanded G<sub>4</sub>C<sub>2</sub> repeat RNA and DPRs are reported to induce nucleocytoplasmic transport defect and nucleolar stress (Freibaum *et al*, 2015; Zhang *et al*, 2015, 2018a; Mizielinska *et al*, 2017), we next asked whether expression of the repeat RNA and DPR affects intracellular localization of EXOSC10. Cells expressing (G<sub>4</sub>C<sub>2</sub>)<sub>80</sub> under strong CMV promoter (Fig 6A) accumulate either

poly-GA, poly-GP, or poly-GR or any combinations of those with poly-GA most abundant (Mori *et al*, 2016). Not all cells with transfected repeat express all the three DPR (Mori *et al*, 2016). In this condition, expression levels of endogenous EXOSC10 were not altered (Fig EV3A–D). To analyze intracellular distribution of EXOSC10, HA-tagged DPR and endogenous EXOSC10 were double-

immunostained. In the analysis, we monitored one of the three DPR species potentially expressed from the RAN translation reporter. This approach could enrich an effect of particular DPR on intracellular distribution of EXOSC10. Interestingly, while EXOSC10

physiologically accumulates in nucleolus (Tomecki *et al.*, 2010), cells lacking nucleolar condensation of EXOSC10 were significantly increased among HA-tagged poly-GR but not HA-tagged poly-GA or HA-tagged poly-GP expressing cells (Fig 6C, D, E, G and H). To test

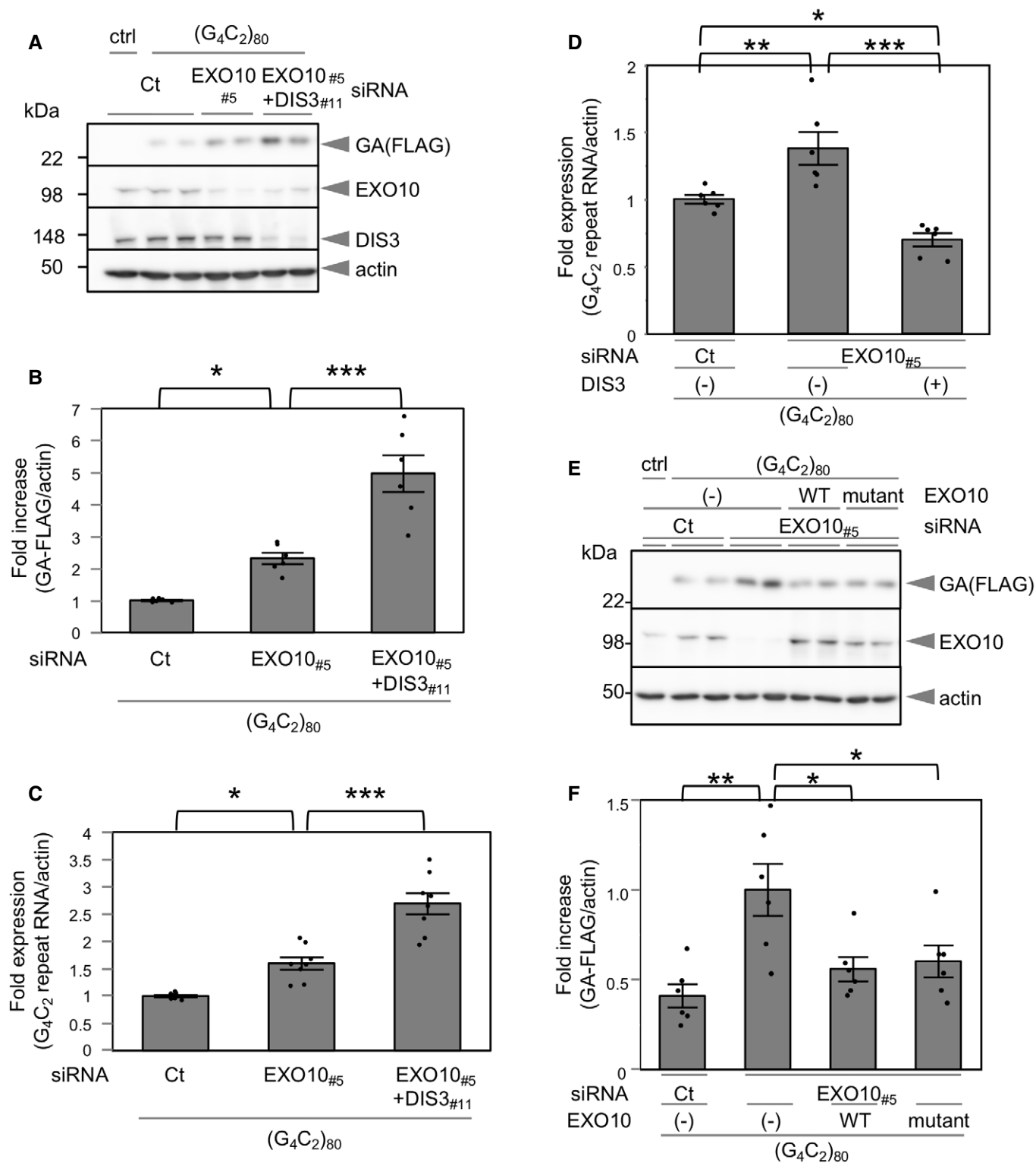


Figure 5.



**Figure 5. DIS3 compensates repeat RNA degradation in the absence of EXOSC10.**

A–C Double knockdown of EXOSC10 and DIS3 significantly increased poly-GA and repeat RNA expression compared with single knockdown of EXOSC10 in cells expressing (G<sub>4</sub>C<sub>2</sub>) 80 repeats. 3 independent experiments. Each experiment performed in duplicates.

D Overexpression of DIS3 compensated EXOSC10 knockdown-induced repeat RNA accumulation. 3 independent experiments. Each experiment performed in duplicates.

E, F Catalytically dead mutant EXOSC10 rescued EXOSC10 knockdown-induced GA increase. 3 independent experiments. Each experiment performed in duplicates.

Data information: All graphs are shown as mean ± SEM. \**P* < 0.05, \*\**P* < 0.01, \*\*\**P* < 0.001; ANOVA with Turkey–Kramer's post-test (B, C, D, F). A dot in graph represents a data point from single well of cell culture plate. Ct: non-targeting siRNA. EXO10<sub>#5</sub>: an siRNA targeting EXOSC10. DIS3<sub>#11</sub>: an siRNA targeting DIS3. "(–)" indicates mock transfection of backbone vector.

Source data are available online for this figure.

the effect of another arginine-rich DPR from antisense repeat strand, poly-proline-arginine (PR), we overexpressed 30 repeats of antisense C<sub>4</sub>G<sub>2</sub> ((C<sub>4</sub>G<sub>2</sub>)<sub>30</sub>) (Fig 6B) in cells (Fig 6F). Again, endogenous expression levels of EXOSC10 were not changed (Fig EV3E and F). Like poly-GR expressing cells, HA-tagged poly-PR expressing cells showed diffuse nuclear misdistribution of EXOSC10 (Fig 6F and I). Taken together, these results suggest arginine-rich DPRs (poly-GR and poly-PR) expressed from G<sub>4</sub>C<sub>2</sub> and C<sub>4</sub>G<sub>2</sub> repeat contribute to the dysregulated distribution of EXOSC10.

**Arginine-rich DPR interacts with EXOSC10 and inhibits G<sub>4</sub>C<sub>2</sub> repeat RNA metabolism in a cellular model of C9orf72 FTL/ALS**

Because multiple components of the RNA exosome complex are among the extended list of poly-GR or poly-PR interactome (Lopez-Gonzalez *et al*, 2016; Boeynaems *et al*, 2017), we next asked whether endogenous EXOSC10 binds to arginine-rich DPRs. First, nuclear and cytoplasmic fractions of cells expressing GFP only or GFP fused with codon optimized versions of DPR [each of poly-GA<sub>89</sub>, GR<sub>89</sub>, PR<sub>89</sub> (Fig 7A)] were obtained. Cells with these constructs express GFP-fused DPR from conventional translation through Kozak sequence and ATG-initiation codon. Optimal nuclear/cytoplasmic separation was validated with Western blot using antibodies against HDAC1 (nuclear marker) and GAPDH (cytoplasmic marker) (Fig 7B). In our system, GFP-poly-PR<sub>89</sub> selectively accumulates within nuclear fraction, while GFP, GFP-poly-GA<sub>89</sub> and poly-GR<sub>89</sub> are distributed throughout nucleus and cytoplasm (Fig 7C and E). The nuclear or cytoplasmic fractions were served for immunoprecipitation using GFP-trap beads. Western blot analysis revealed that in cytoplasmic fraction where GFP-poly-PR<sub>89</sub> is absent, EXOSC10 accumulated only in GFP-poly-GR fraction (Fig 7C and D). In nuclear fraction, EXOSC10 are selectively detected in GFP-poly-GR<sub>89</sub> and GFP-poly-PR<sub>89</sub> precipitants but not in

control GFP only or GFP-poly-GA<sub>89</sub> precipitants (Fig 7E and F). Expression levels of EXOSC10 were not altered by the presence of GFP-poly-GR<sub>89</sub>, GFP-poly-PR<sub>89</sub>, and GFP-poly-GA<sub>89</sub> (Fig EV4A and B). These results suggest preferential binding of EXOSC10 with arginine-rich DPRs, and such interaction may contribute functional impairment of the RNA exosome complex.

To examine whether arginine-rich DPRs indeed alter intracellular RNA metabolism through EXOSC10, we analyzed endogenous substrates of EXOSC10: short 3'extended snoRA48 and snoRA68 precursors (Davidson *et al*, 2019). To do so, qPCR primers targeting 3'extended region of snoRNAs were designed. First, we confirmed that EXOSC10 knockdown increased the expression of endogenous 3'extended snoRA48 and snoRA68 precursors (Fig 8B and D). This verified these snoRNA precursors are indeed substrates of EXOSC10. Importantly, GFP-poly-GR<sub>177</sub> or GFP-poly-PR<sub>166</sub> expression augmented expressions of these snoRNA precursors (Fig 8A, C and E). These results suggest arginine-rich DPR causes functional impairment of EXOSC10. To further validate our model that GR/PR inhibits EXOSC10-dependent repeat RNA degradation, we co-expressed EF1 promoter-based (G<sub>4</sub>C<sub>2</sub>) 80 repeats and each of GFP-fused arginine-rich DPRs (Figs 1A and 8A, and EV4C–G). Strikingly, the expression of GFP-poly-GR<sub>177</sub> or GFP-poly-PR<sub>166</sub> induced augmented accumulation of G<sub>4</sub>C<sub>2</sub> repeat RNA (Fig 8F). Together, these results indicate that arginine-rich DPR impedes C9orf72 repeat RNA metabolism through the inhibition of EXOSC10/the RNA exosome complex.

**Discussion**

Here, we have shown the RNA exosome complex confers degradation of expanded G<sub>4</sub>C<sub>2</sub> repeat RNA in C9orf72 FTL/ALS. The repeat RNA could be toxic by itself through sequestration of specific RNA

**Figure 6. Arginine-rich DPR modulates intracellular distribution of endogenous EXOSC10.**

A, B HeLa cells were transfected with one of the G<sub>4</sub>C<sub>2</sub> repeat plasmids (A), antisense C<sub>4</sub>G<sub>2</sub> repeat plasmid (B), or control mock plasmid. "mock" indicates a control vector which lacks the repeat but still contains the 5' flanking region and 3xTAG.

C–F HA-tagged poly-GA, poly-GP, poly-GR or poly-PR (red), and EXOSC10 (green) were immunostained with anti-HA and anti-EXOSC10 antibodies. Nuclei were stained with DAPI (blue). Scale bar = 10 μm.

G EXOSC10 (green) was immunostained with anti-EXOSC10 antibody in cells transfected with control mock plasmid. Nuclei were stained with DAPI (blue). Scale bar = 10 μm.

H, I Quantification of the frequency of cells with mislocalized EXOSC10. Only DPR-positive cells were quantified (except mock-transfected cells expressing no DPR. In this case, all cells in the picture were quantified). 3 independent experiments. (Total cell counts: (H) mock 300 cells, GA 112 cells, GP 69 cells, GR 53 cells, (I) mock 445 cells, PR 159 cells).

Data information: All graphs are shown as mean ± SEM. \*\**P* < 0.01, \*\*\**P* < 0.001; ANOVA with Dunnett's post-test vs. mock (H) or two-tailed unpaired t-test (I). A dot in graph represents a data from single well of cell culture plate.

Source data are available online for this figure.

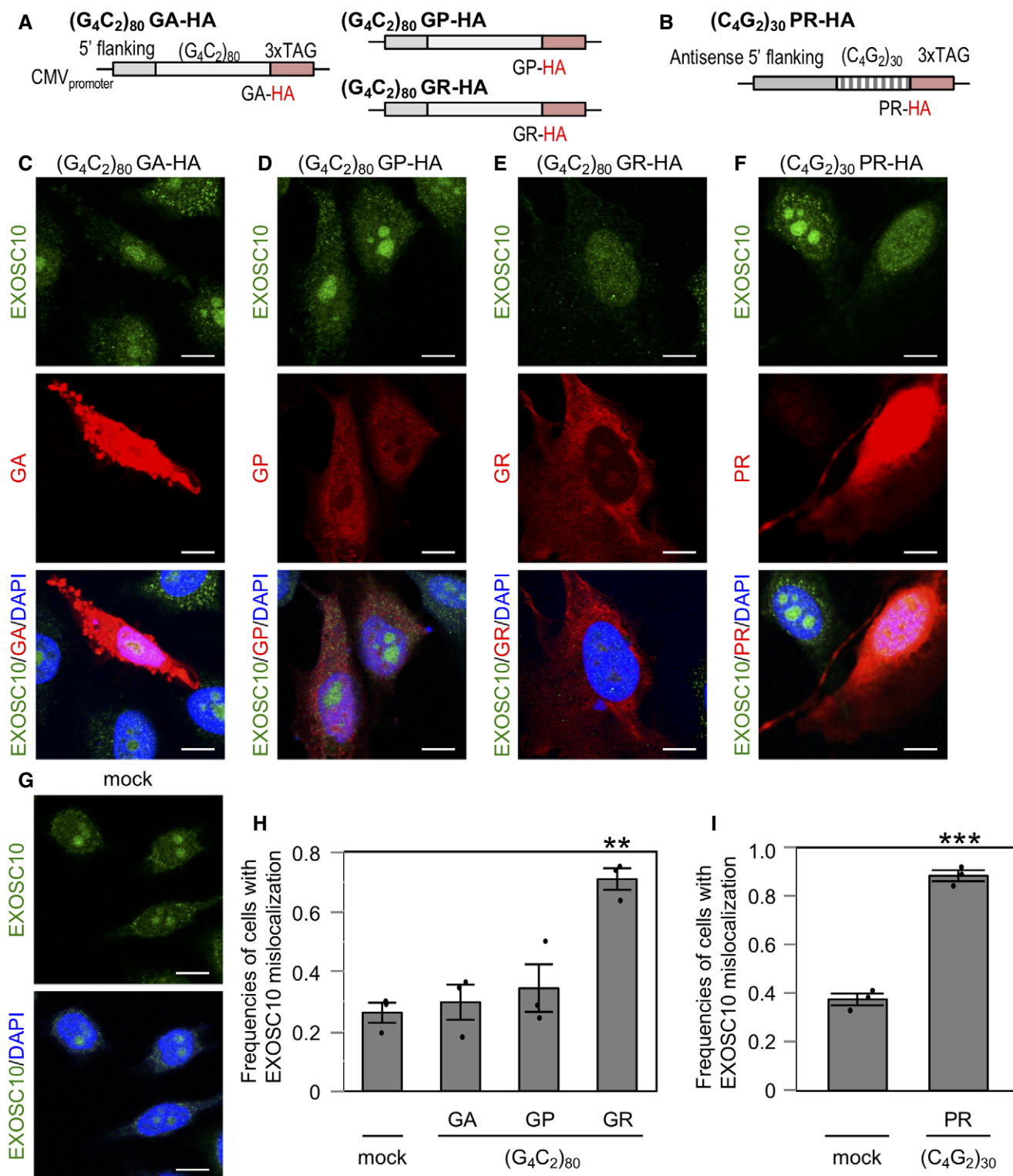


Figure 6.

binding proteins (Donnelly *et al*, 2013; Lee *et al*, 2013; Mori *et al*, 2013b; Sareen *et al*, 2013; Xu *et al*, 2013; Cooper-Knock *et al*, 2014). Especially, association between antisense RNA foci and TDP-43 pathology has been reported (Cooper-Knock *et al*, 2015;

Aladesuyi Arogundade *et al*, 2019). At the same time, the repeat RNA is a source of highly toxic DPRs (Mori *et al*, 2013c; May *et al*, 2014; Mizielinska *et al*, 2014; Zhang *et al*, 2016, 2018b). Therefore, reduction of the repeat RNA could potentially be therapeutic option

in *C9orf72* FTL/D/ALS. In our condition, EXOSC10 is most relevant to the repeat RNA metabolism among the three catalytic subunits of the RNA exosome complex [i.e., EXOSC10, DIS3, and DIS3L (Allmang et al, 1999b; Mitchell et al, 1997; Tomecki et al, 2010)]. Reduced EXOSC10 increases the levels of the repeat RNA which leads to elevated DPR production and accumulation. Not surprisingly, these effects were canceled by exogenous expression of

EXOSC10. *In vivo* RNA stability assay using transcription inhibitor actinomycin D confirmed EXOSC10 knockdown compromised both sense and antisense repeat RNA degradation. Moreover, recombinant EXOSC10 efficiently degrades synthetic sense and antisense repeat RNA. These results strongly support EXOSC10-mediated degradation of *C9orf72* repeat RNA. Crucially, in fibroblast derived from patients with *C9orf72* repeat expansion, we confirmed an

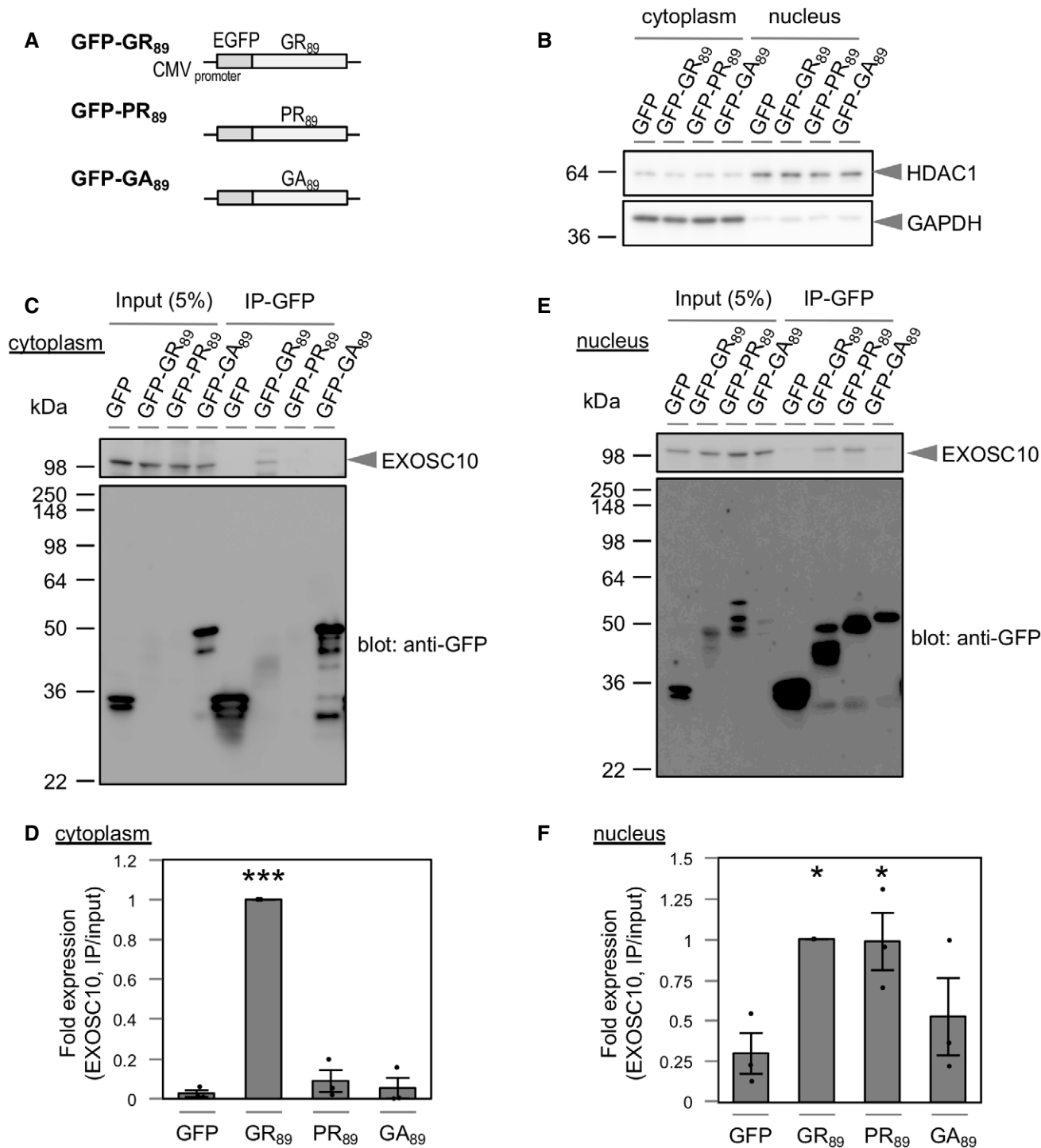


Figure 7.

**Figure 7. Arginine-rich DPRs have preferential interaction with endogenous EXOSC10.**

- A Schematic diagrams of codon optimized (lacking extensive  $G_4C_2$  repeat) plasmids expressing N-terminally EGFP fused 89 repeats of either poly-GR, poly-PR, or poly-GA under the control of CMV promoter.
- B Immunoblot validation of successful fractionation using antibodies against HDAC1 (nuclear marker) and GAPDH (cytoplasmic marker).
- C Co-immunoprecipitation of GFP-DPR interacting proteins in cytoplasmic fraction using GFP-trap beads. Immunoprecipitants were served for immunoblot with anti-EXOSC10 antibody. The same membrane was reprobed with anti-GFP antibody.
- D Quantification of the relative intensities of "EXOSC10 in co-IP fraction"/"EXOSC10 in input". 3 independent experiments.
- E Co-immunoprecipitation of GFP-DPR interacting proteins in nuclear fraction using GFP-trap beads followed by immunoblot using anti-EXOSC10 antibody. The same membrane was reprobed with anti-GFP antibody.
- F Quantification of the relative intensities of "EXOSC10 in co-IP fraction"/"EXOSC10 in input". 3 independent experiments.

Data information: All graphs are shown as mean  $\pm$  SEM. \* $P < 0.05$ , \*\*\* $P < 0.001$ ; ANOVA with Dunnett's post-test vs. GFP (D, F). A dot in graph represents a data point from single well of cell culture plate.

Source data are available online for this figure.

accumulation of both sense and antisense RNA foci and repeat RNA transcripts upon EXOSC10 knockdown. This implicates *in vivo* relevance of EXOSC10 in *C9orf72* FTL/ALS context. *In vivo* and *in vitro* RNA degradation assays differ in the enzymatic composition. In *in vivo* assay, EXOSC10 is expected to work as a component of the RNA exosome complex, while *in vitro* assay we used recombinant EXOSC10 alone as a catalytic machinery. The antisense repeat RNA may be slightly more resistant to EXOSC10-mediated degradation *in vivo* (Figs 3A and B, and 4F and G) and *in vitro* (Fig 3C–F). Reported structural difference between sense and antisense repeat RNA might underlie the observed difference (Fratta *et al*, 2012; Reddy *et al*, 2013; Haeusler *et al*, 2014; Dodd *et al*, 2016).

Although less prominent, DIS3 is also significantly involved in the degradation of repeat RNA. An additive knockdown of DIS3 on EXOSC10 knockdown boosted repeat RNA and DPR expression. Moreover, DIS3 overexpression compensated EXOSC10 knockdown-induced repeat RNA accumulation. These results argue that the RNA exosome complex as a whole works as a  $G_4C_2$  and  $C_4G_2$  repeat RNA degradation machinery. EXOSC10 has the two proposed functions on RNA degradation. One is RNase activity of its own, and another is promotion of substrate loading into tunnel of the barrel-like core of the RNA exosome complex. Mechanistically, we found even the catalytically dead version of EXOSC10 can rescue EXOSC10 knockdown-induced GA increase, possibly through facilitating RNA degradation by DIS3. This suggests EXOSC10's promotion of substrate loading plays significant role in repeat RNA degradation. However, EXOSC10's own 3'exoribonuclease catalytic activity should not be ignored. One reason is because single knockdown of DIS3 did not affect GA expression (Fig 1C). Since DIS3 knockdown is expected to cancel the consequence of EXOSC10's substrate

loading effect, catalytic activity of EXOSC10 seems to have ability to compensate it. Another argument is that we did confirm repeat RNA degradation with purified EXOSC10 via its 3'exoribonuclease activity *in vitro*. These findings suggest both EXOSC10's inherent RNase activity and substrate loading activity works in cooperative manner in the context of repeat RNA degradation.

We found intranuclear localization of EXOSC10 is misregulated in cells expressing arginine-rich DPRs in a RAN translation-dependent manner. Because cells with the RAN translation reporter construct express repeat RNA potentially together with single to multiple DPR species in a various combination, we could not exclude the possibility that observed mislocalization in arginine-rich DPR expressing cells is due to compound effects of arginine-rich DPR and co-expressed repeat RNA/the other DPRs. Still, frequency of cells with EXOSC10 mislocalization was significantly increased in cells selected with arginine-rich DPR positivity compared with that of control mock-transfected cells, but not in cells selected with poly-GA or GP positivity (Fig 6). This finding implicates the potential importance of arginine-rich DPR in EXOSC10 mislocalization. Since *C9orf72* repeat RNA and DPRs are known to induce nucleocytoplasmic transport defect and nucleolar stress, mislocalization of EXOSC10 could be the downstream effect of these cellular dysregulation. Mislocalization of EXOSC10 may cause its functional impairment; however, at the moment we have no direct evidence on this point. In accord with recent reports of DPR interactome (Lopez-Gonzalez *et al*, 2016; Boeynaems *et al*, 2017), we confirmed that arginine-rich DPRs have preferential interaction with endogenous EXOSC10. The EXOSC10-DPR interactions may cause functional impairment of the RNA exosome complex. Indeed, 3'extended snoRA48 and snoRA68 precursors,

**Figure 8. Arginine-rich DPR causes functional impairment of EXOSC10/the RNA exosome complex.**

- A Schematic diagrams of codon optimized (lacking extensive  $G_4C_2$  repeat) plasmids expressing N-terminally EGFP fused 177 repeats of poly-GR or 166 repeats of poly-PR under the control of CMV promoter.
- B, C Increased expression of 3'extended snoRA48 precursor upon EXOSC10 knockdown (B) or GFP-poly-GR<sub>177</sub>/GFP-poly-PR<sub>166</sub> expression (C) on RT-qPCR. 6 independent experiments. Each experiment performed in duplicates.
- D, E Increased expression of 3'extended snoRA68 precursor upon EXOSC10 knockdown (D) or GFP-poly-GR<sub>177</sub>/GFP-poly-PR<sub>166</sub> expressions (E) on RT-qPCR. 6 independent experiments. Each experiment performed in duplicates.
- F RT-qPCR analysis showed increased cellular  $G_4C_2$  repeat RNA expression from co-transfected EF1 ( $G_4C_2$ )<sub>80</sub> repeat construct (Fig 1A) in the presence of GFP, GFP-poly-GR<sub>177</sub>, or GFP-poly-PR<sub>166</sub>. 3 independent experiments. Each experiment performed in duplicates.

Data information: All graphs are shown as mean  $\pm$  SEM. \* $P < 0.05$ , \*\* $P < 0.01$ , \*\*\* $P < 0.001$ ; two-tailed unpaired t-test (B, D) or ANOVA with Dunnett's post-test vs. GFP (C, E, F). A dot in graph represents a data point from single well of cell culture plate.

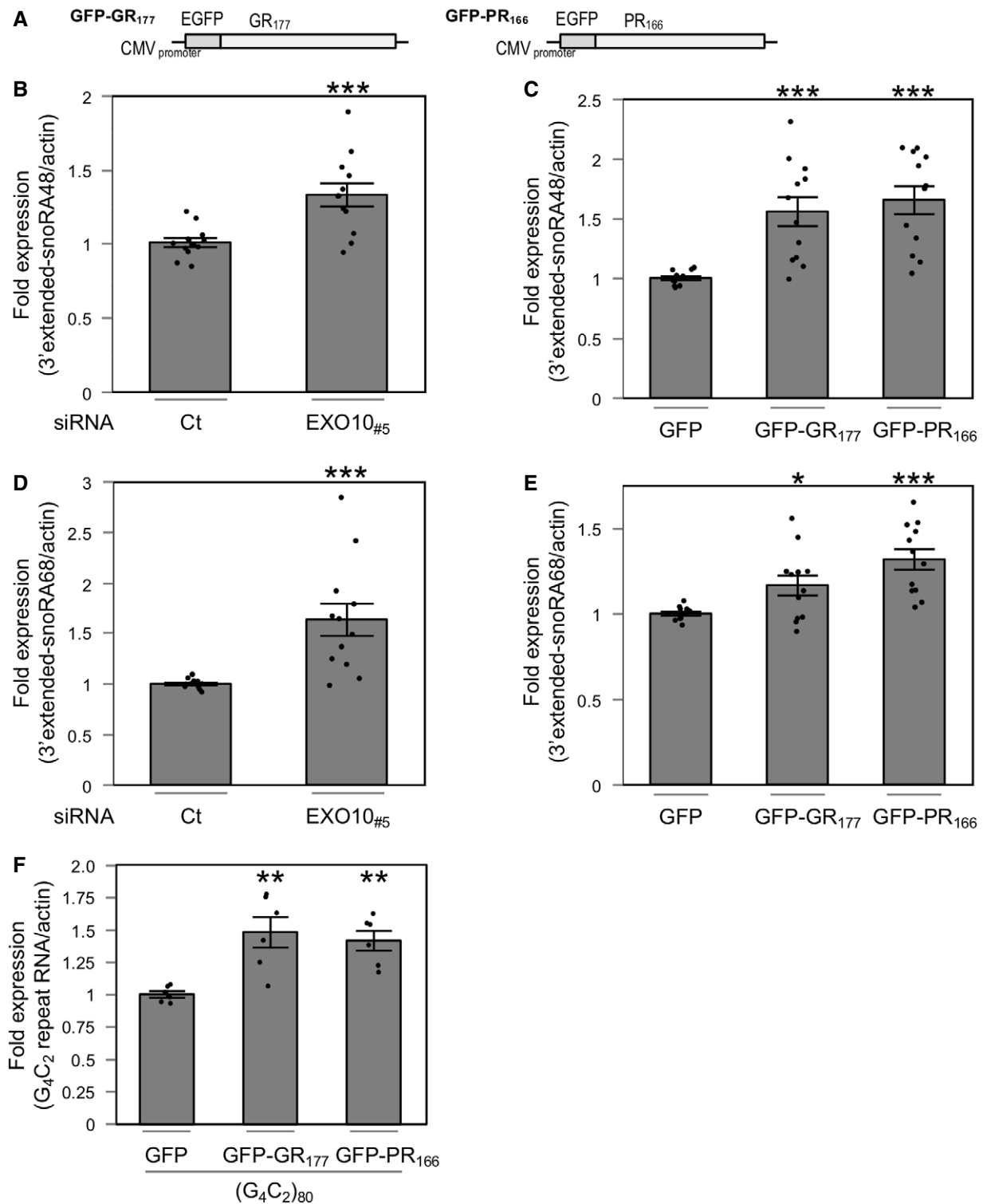
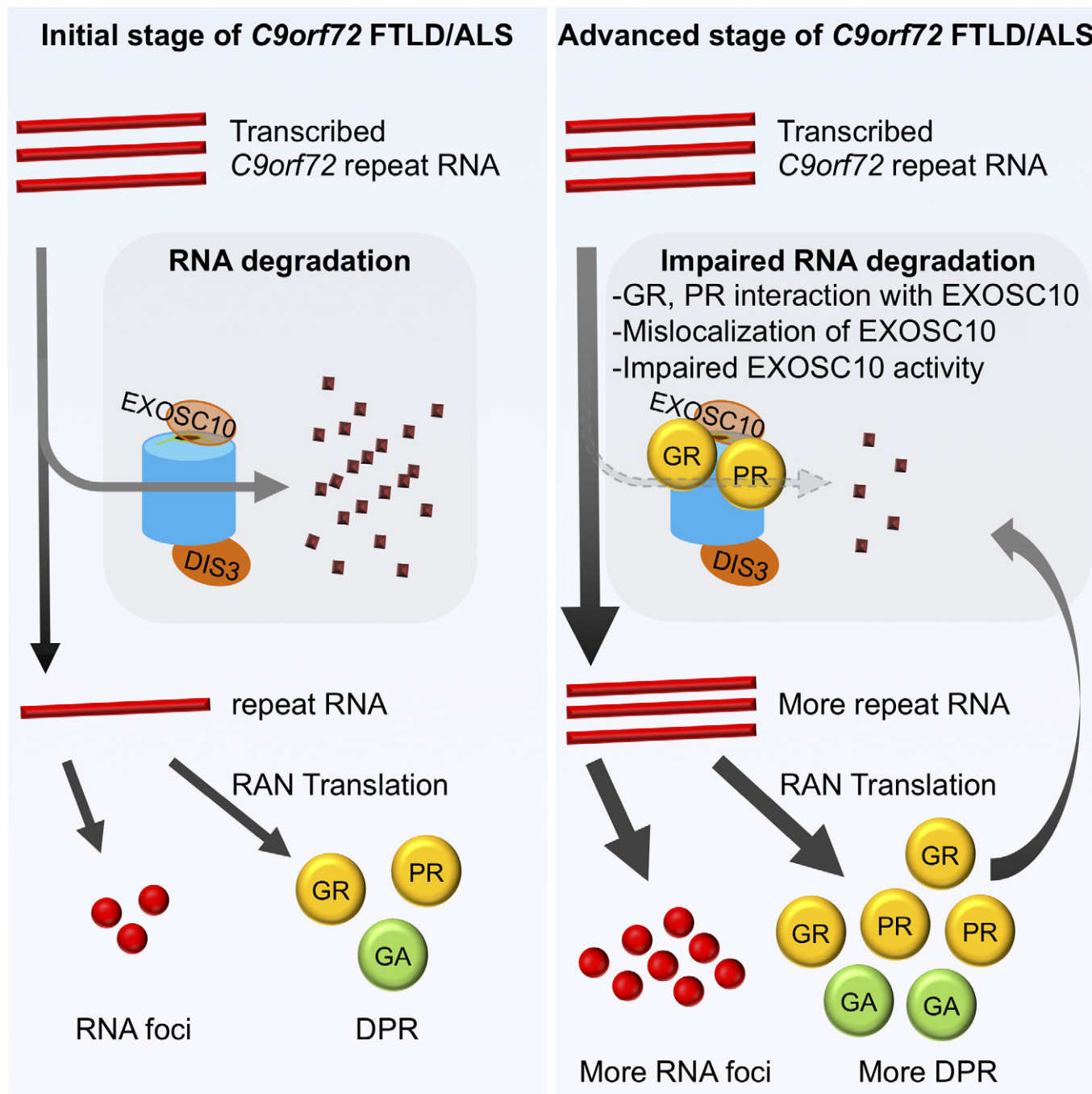


Figure 8.

previously reported as endogenous substrates of EXOSC10, accumulated in poly-GR and poly-PR expressing cells. Moreover, the expression of G<sub>4</sub>C<sub>2</sub> repeat RNA is significantly increased when co-expressed with poly-GR or poly-PR. Thus, it is tempting to speculate that DPR-mediated functional impairment of the RNA

exosome complex leads to impaired nuclear RNA quality surveillance and thus accumulation of unusual repeat RNA (Fig 9). Interestingly, a recent report revealed repetitive element transcripts are elevated in the brain of *C9orf72* ALS/FTD patients (Prudencio *et al*, 2017). Since the repeat RNA transcripts escaped from



**Figure 9. Conceptual summary.**

Impairment of EXOSC10 with arginine-rich DPR compromises repeat RNA degradation through the RNA exosome complex. This accelerates repeat RNA accumulation (as RNA foci) and RAN translation-dependent DPR production. The produced DPR in turn compromises EXOSC10/the RNA exosome complex and thus accelerates the pathological process of *C9orf72* FTL/ALS.

nuclear RNA quality surveillance can accumulate as RNA foci or even exported to cytoplasm where it would be translated into DPR, DPR-mediated functional impairment of the RNA exosome complex may lead to inefficient metabolism of the repeat RNA and further accumulation of DPR. Consequently, this pathological downward spiral may exacerbate neurodegeneration in *C9orf72* FTL/ALS.

## Materials and Methods

### Cell culture

HeLa cells were cultured in DMEM containing 10% FCS and penicillin/streptomycin (P/S). SH-SY-5Y cells were cultured in DMEM/F-12 containing 10% FCS and P/S.

## Patient-derived fibroblasts

We used fibroblast cell lines from three different *C9orf72* ALS cases. These cells were originally obtained based on written informed consent in accordance with the Helsinki convention as previously described (Mori *et al*, 2016; Zhou *et al*, 2017). Cells were grown in DMEM supplemented with 20% FCS and P/S. The presence of the expanded *C9orf72* repeat was confirmed by repeat prime PCR (Aki-moto *et al*, 2014).

## Plasmids

The EF1 promoter-driven and CMV promoter-driven ( $G_4C_2$ ) 80 repeats vectors are described previously (Mori *et al*, 2013c, 2016). CMV promoter-driven ( $C_4G_2$ ) 30 repeats vector is described previously (Nihei *et al*, 2020). EXOSC10 coding sequence was subcloned from pT7-V5-SBP-C1-HsRRP6 (Addgene plasmid # 64916, a gift from Prof. Elisa Izaurralde) into HindIII/BamHI site of the pcDNA3.1 hygro (+) vector (Invitrogen). To generate a siRNA-resistant EXOSC10, several silent mutations in siRNA target sequence (J-010904-05 Human EXOSC10 ACGAAAAGCUCUUGAAUUG) were introduced by site-directed mutagenesis inverse PCR using primers CTGAACTGCCAGGAATTTGCAGTTGACTTG and CAGTTTTTCATTGAGTTCCACGAGTTCATC. To generate a catalytically dead version of EXOSC10 (triple point mutations; D313N + D371N + E315Q), we performed sequential site-directed mutagenesis. Point mutation was introduced using the following primers: TGCCAGGAATTTGCAGT-TAACTTGGAGCACCCTCT and AGAGTGGTGTCTCAAGTAAAC TGCAAATTCCTGGCA for D313N, GGTCTTTCATGGTGCTGATTC AACATAGAAATGGCTACAG and CTGTAGCCATTCTATGTTTGAA TCAGCACCATGAAAGACC for D371N, GAATTTGCAGTAACTTGC AGCACCACTTACAGGAGC and GCTCCTGTAAGAGTGGTGCTG CAAGTTAACTGCAAATTC for E315Q. Human DIS3 was cloned into pcDNA3.1hygro(+) vector (Invitrogen) at BamHI/NotI sites. Coding sequence was obtained through nested PCR using cDNA from HeLa cells and following primer sets. (1<sup>st</sup> PCR: CTCGGGGTTAGGC GTATTC and CCCTGAAGTTGCTGCTCTGT, 2<sup>nd</sup> PCR: CGCGGATCC GCCACCATGCTCAAGTCCAAGACGTTTC and CGCGCGCCGCT ATTTTCCAAGCTTCATCTTC). Sequence was verified with Sanger sequence.

pEGFP-GR<sub>89</sub>, PR<sub>89</sub>, GA<sub>89</sub>, GR<sub>177</sub>, and PR<sub>166</sub> vectors were constructed as previously described (Bennion Callister *et al*, 2016) with slight modifications (Nihei *et al*, 2020). DNA oligo coding 12 repeats of each DPR, but avoiding GGGGCC or CCCC GG repeat sequence, were designed using alternative codons. Restriction sites for XhoI-FokI and BbsI-XbaI were placed at the beginning and end of the oligo DNA. The codon optimized 11 repeat coding DPR sequences were isolated through digestion with FokI and BbsI and then ligated into BbsI-linearized parental 12 repeat DPR coding vector to double the repeat length. This process was repeated until reached 177 repeat lengths were achieved (12 + 11 = 23 repeats, 23 + 22 = 45 repeats, 45 + 44 = 89 repeats, 89 + 88 = 177 repeats). We failed to obtain PR<sub>177</sub> due to instability of repetitive sequence during cloning. DNA sequence was verified by Sanger sequence.

XhoI-FokI-GA12-BbsI-XbaI: 5'-CTCGAGGGATGTTGAATTCTGGTCTGGCGCGGGAGCAGGCGCTGGTGTGGTGCAGGAGCGGGTCCGGGAGCTGGTGCCGGCGCAGGTGCTGTCTTCGGATCCTAGTCTAGA-3'

XhoI-FokI-GR12-BbsI-XbaI: 5'-CTCGAGGGATGTTGAATTCTGGTCTGGACGTGGACGAGGTCGAGGTCGAGGTCGTGGACGTGGTCCGAGTTCGAGGTCGTGGACGTGGTCTGTCTTCGGATCCTAGTCTAGA-3'

XhoI-FokI-PR12-BbsI-XbaI: 5'-CTCGAGGGATGTTGAATTCTCCGCGACCTCGACCGCGCCACGCCACGCCCTCGGCCAGACCACGTCCTAGGCCAGACCCAGACCGCGAGTCTTCGGATCCTAGTCTAGA-3'

## siRNA-mediated knockdown and plasmid transfection

The following siRNAs were obtained from Dharmacon: ON-TARGETplus Human non-targeting siRNA D-001810-01, J-010904-05 Human EXOSC10 ACGAAAAGCUCUUGAAUUG, J-010904-07 Human EXOSC10 GAAGUGACAUGUACAUUCU, J-015405-11 Human Dis3 UGAUGAAGAUCGUGCGCGA, J-015405-12 Human Dis3 AGGUAGA GUUGUAGGAAUA, J-015333-05 Human Dis3L GAACAAGGGCCAC CACUUA, J-015333-06 Human Dis3L UGACGGAGUUAUUUAUUCA. Five or ten picomoles of each siRNA was reverse-transfected using RNAiMax (Thermo Fisher Scientific) and OPTI-MEM when 24-well plate format was used. After overnight incubation, media were exchanged and 1 ng/μl (500 μl when 24-well plate format is used) of plasmids was transfected with lipofectamine LTX with plus reagent (Thermo Fisher Scientific) in OPTI-MEM into HeLa cells unless otherwise stated. On SH-SY5Y cells, lipofectamine 3000 with P3000 reagent (Thermo Fisher Scientific) in OPTI-MEM was used alternatively. For rescue experiments, 1 ng/μl of repeat expressing plasmids and 0.006, 0.02, 0.06, and 0.2 ng/μl for dose-response experiment, and 0.2 ng/μl for single dose experiment of rescue constructs were co-transfected. Media were exchanged after 4- to 6-h incubation. Cells were harvested 2 days after plasmid transfection for Western blot unless otherwise indicated.

## Antibodies

The following antibodies were used for Western blots (WB), immunofluorescence (IF), and Filter trap (FT): anti-DYKDDDDK (FLAG) Tag (Cell Signaling #2368S) WB 1/1,000, anti-myc clone 9E10 (Santa Cruz) WB 1/1,000, IF 1/100, anti-HA Tag clone 3F10 (Roche) WB 1/1,000, IF 1/100, anti-GFP(B-2) (Santa Cruz) WB 1/500, FT 1/500, anti-beta-actin (Sigma-Aldrich) WB 1/1,000, FT 1/1,000, anti-EXOSC10 (ATLAS ANTIBODIES) WB 1/500, IF 1/2,000, anti-DIS3 (Proteintech) WB1/2,000, anti-DIS3L (Santa Cruz) WB 1/500, anti-GAPDH (Proteintech) WB 1/20,000, anti-HDAC1 (Proteintech) 1/1,000, anti-PR (Proteintech) WB 1/500, FT 1/500, anti-GR (Proteintech) WB 1/1,000, FT 1/1,000.

## Reverse transcription and quantitative polymerase chain reaction (RT-qPCR)

HeLa cells expressing ( $G_4C_2$ )<sub>80</sub> or ( $C_4G_2$ )<sub>30</sub> repeats were harvested 1–2 days after plasmid transfection. Total RNA was prepared using the RNeasy and Qiashredder kit (Qiagen). RNA preparations were treated with Turbo DNA-free kit (Thermo Fisher Scientific) to minimize residual DNA contamination. Two micrograms of RNA was used for reverse transcription with M-MLV Reverse Transcriptase (Promega) using oligo-(dT) 12–18 primer (Invitrogen). RT-qPCR was performed using the ViiA7 Real-Time PCR System (Applied Biosystems) with TaqMan technology. Primers and probes were designed (IDT) for 3' TAG region of repeat constructs (repeat TAG

primer for sense repeat). Primer 1: TCT CAA ACT GGG ATG CGT AC, Primer 2: GTA GTC AAG CGT AGT CTG GG, Probe/56-FAM/TG CAG ATA T/Zen/C CAG CAC AGT GGC G/3IABkFQ/. For antisense repeat primer and probe set (C4G2 antisense tag) were used. Primer 1: TCT CAA ACT GGG ATG CGT, Primer 2 GTC CTT GTA GTC AAG CGT AGT C, Probe/56-FAM/TC GTA TGG G/Zen/T ACC CGG GTT TGC/3IABkFQ/. A primer/probe set for Human ACTB, Hs.PT.39a.22214847 (IDT) was used as endogenous control. Each sample was paired with no reverse transcription controls showing  $< 1/2^{10}$  ( $\Delta\Delta C_T > 10$ ) signal when compared to reverse transcribed samples, thus excluding contamination of plasmid DNA-derived signal. Each biological sample (=a sample from a well of culture plate) was analyzed in duplicate or triplicate. Signals of repeat RNA-derived cDNA were normalized to ACTB cDNA according to the  $\Delta\Delta C_T$  method. Alternatively, patient-derived fibroblasts were harvested 3 days after siRNA-mediated knockdown. For the strand-specific quantification of endogenous repeat RNA in fibroblast, total RNA was collected as described above. 3' proximity region of endogenous G<sub>4</sub>C<sub>2</sub> repeat was targeted for RT-qPCR as previously described (Mori *et al*, 2013c). SuperScript IV Reverse Transcriptase (Thermo Fisher Scientific) and strand-specific primers (either sense RT primer CAATTCCACGATCGCTAGA or antisense RT primer CTGCGGTTGCGGTGCCTGC) were used for strand-specific reverse transcription. The following set was used for qPCR; Primer 1: AAG AGG CGC GGG TAG AA, Primer 2: CAG CTT CGG TCA GAG AAA TGA G, Probe: /56-FAM/CT CTC CTC A/Zen/G AGC TCG ACG CAT TT/3IABkFQ/ (Mori *et al*, 2013c). Obtained signals were normalized according to the  $\Delta C_T$  method. PCR product was validated by Sanger sequencing.

#### RT-qPCR for 3'ext-snoRA48, 68

HeLa cells were harvested 2 days after siRNA-mediated knockdown or 1 days after plasmid transfection (GFP, GFP-GR<sub>177</sub>, GFP-PR<sub>166</sub>). Total RNA was extracted and analyzed as described above except random hexamer (Invitrogen) was used for reverse transcription. The following set was designed and used for 3'ext-snoRA48, Primer 1: CAA AGC AAC TCC TTG TTC ATC C, Primer 2: GGC TAC AAT ACC ACC TCT TTA AAG, Probe/56-FAM/TG GTT CAT G/Zen/C CTT GGA CAC ATA GGT/3IABkFQ/; and for 3'ext-snoRA68, Primer 1: GCA AAC AGC AAG CGG ATC TT, Primer 2 CCC TGC AGT CAC TGG CC, Probe/56-FAM/CC CTC AAA G/Zen/T GAA TTT GGA GGT TCC ACA/3IABkFQ/. PCR product was validated by Sanger sequencing.

#### In vivo RNA stability assay using Actinomycin D

HeLa cells were cultured on 12-well culture plates and reverse-transfected with indicated siRNAs (non-targeting control or targeting EXOSC10) (day 0). The next day cells were transfected with repeat plasmid for 6 h (day 1). On day 2, 10  $\mu\text{g/ml}$  actinomycin D pretreatment was started at time point  $-1$  h to abolish transcription. In the presence of actinomycin D, cells were then sequentially collected at indicated time points (0, 0.5, 1, 2, and 3 h) and frozen immediately. Since actinomycin D treatment may drastically affect total amount/composition of cellular RNA, equal amount of *in vitro* transcribed EGFP RNA using RiboMAX Large Scale RNA Production System-T7 (Promega) was added each well just prior to RNA purification as a normalization control. Total RNA was extracted and analyzed as

described in RT-qPCR section. The following set was used for qPCR targeting EGFP, Primer 1: GCA CAA GCT GGA GTA CAA CTA, Primer 2: TGT TGT GGC GGA TCT TGA A, Probe: /56-FAM/AG CAG AAG A/Zen/A CGG CAT CAA GGT GA/3IABkFQ/ qPCR signals of repeat RNA-derived cDNA were normalized for time point 0 h, and normalized expressions of repeat RNA/EGFP are shown according to the  $\Delta\Delta C_T$  method.

#### In situ hybridization

*In situ* hybridization was performed as previously described (Mori *et al*, 2016) with slight modifications. 4% paraformaldehyde-fixed and 0.2% Triton X-100 perforated cells on glass coverslips were rinsed 2 $\times$  SSC and then incubated in prehybridization solution (40% formamide (Life Technologies, 15515-026), 2 $\times$  SSC, 2.5% BSA) at 57°C for 30 min. Cells were then incubated with hybridization solution (40% formamide, 2 $\times$  SSC, 0.8 mg/ml tRNA (Roche), 0.8 mg/ml single strand salmon sperm DNA (Sigma-Aldrich, D7656), 0.16% BSA, 8% Dextran sulfate (Sigma-Aldrich), 1.6 mM Ribonucleoside-vanadyl complex (New England Biolabs, S1402S), 5 mM EDTA, 100 ng (for HeLa), or 10 ng (for Fibroblasts)/ml 5' Cy3-labeled (CCCCGG)  $\times$  4 probe or 5' Cy3-labeled (GGGGCC)  $\times$  4 probe (IDT; DeJesus-Hernandez *et al*, 2011) at 57°C (for sense foci) or at 37°C (for antisense foci) overnight. The following day, cells were sequentially washed in 40% formamide, 0.5 $\times$  SSC for three times 10 min each at 57°C and then with 0.5 $\times$  SSC three times 10 min each at room temperature. After a brief rinse with PBS, cells were washed 0.05% Tween20 in 1 $\times$  PBS for three times 5 min each. Nuclei were counterstained with 0.1  $\mu\text{g/ml}$  of DAPI for 20 min and then washed with 0.05% Tween20 in 1 $\times$  PBS for three times 5 min each. Glass coverslips were mounted using Prolong Diamond antifade (Life Technologies) and analyzed with Leica DMI400B confocal microscopy with LAS AF software (Leica). For quantification of RNA foci on fibroblast, cells were analyzed with LSM710 (Zeiss) microscope with a 63 $\times$ /1.20 W Korr M27 oil immersion objective. Z-Stacked images of 1  $\mu\text{m}$  thickness were sequentially taken to cover the whole nucleus at 4.0 times digital zoom. Number of RNA foci within DAPI-positive area was manually counted at 3D presentation at Maximum projection mode using Zen2011 software (Zeiss).

%cells with RNA foci in HeLa cell were manually counted from RNA foci signals and DAPI signals of single plane images. Quantification of RNA foci intensity in HeLa cells was performed using ImageJ software. Binary images from DAPI counterstaining were used for the nuclear regions. RNA foci intensity of a cell was defined as ["average Cy3 signal in DAPI-positive area of RNA foci-positive cell" subtracted with "average Cy3 signal in DAPI-positive area of RNA foci-negative cell"] times "DAPI-positive area of a RNA foci-positive cell". RNA foci intensities were quantified from three independent experiments.

#### co-IP experiment

HeLa cells expressing GFP or GFP-poly-DPR (GA<sub>89</sub>, GR<sub>89</sub>, PR<sub>89</sub>) were harvested 1 days after plasmid transfection. Cells were lysed and separated into nuclear and cytoplasmic fractions using NE-PER Nuclear and Cytoplasmic Extraction Reagents (Thermo Scientific).

These fractions were incubated with GFP-TRAP A beads (Chromo Tek) overnight at 4°C and subsequently precipitated by





- EXOSC9 disrupt the RNA exosome and result in cerebellar atrophy with spinal motor neuronopathy. *Am J Hum Genet* 102: 858–873
- Cooper-Knock J, Walsh MJ, Higginbottom A, Robin Highley J, Dickman MJ, Edbauer D, Ince PG, Wharton SB, Wilson SA, Kirby J *et al* (2014) Sequestration of multiple RNA recognition motif-containing proteins by C9orf72 repeat expansions. *Brain* 137: 2040–2051
- Cooper-Knock J, Higginbottom A, Stopford MJ, Highley JR, Ince PG, Wharton SB, Pickering-Brown S, Kirby J, Hautbergue GM, Shaw PJ (2015) Antisense RNA foci in the motor neurons of C9ORF72-ALS patients are associated with TDP-43 proteinopathy. *Acta Neuropathol* 130: 63–75
- Davidson L, Francis L, Cordiner RA, Eaton JD, Estell C, Macias S, Caceres JF, West S (2019) Rapid depletion of DIS3, EXOSC10, or XRN2 reveals the immediate impact of exoribonucleolysis on nuclear RNA metabolism and transcriptional control. *Cell Rep* 26: 2779–2791
- DeJesus-Hernandez M, Mackenzie IR, Boeve BF, Boxer AL, Baker M, Rutherford NJ, Nicholson AM, Finch NA, Flynn H, Adamson J *et al* (2011) Expanded GGGGCC hexanucleotide repeat in noncoding region of C9ORF72 causes chromosome 9p-linked FTD and ALS. *Neuron* 72: 245–256
- Dodd DW, Tomchick DR, Corey DR, Gagnon KT (2016) Pathogenic C9ORF72 antisense repeat RNA forms a double helix with tandem C: C mismatches. *Biochemistry* 55: 1283–1286
- Donnelly CJ, Zhang PW, Pham JT, Heusler AR, Mistry NA, Vidensky S, Daley EL, Poth EM, Hoover B, Fines DM *et al* (2013) RNA toxicity from the ALS/FTD C9ORF72 expansion is mitigated by antisense intervention. *Neuron* 80: 415–428
- Drazkowska K, Tomecki R, Stodas K, Kowalska K, Czarnocki-Cieciura M, Dziembowski A (2013) The RNA exosome complex central channel controls both exonuclease and endonuclease Dis3 activities *in vivo* and *in vitro*. *Nucleic Acids Res* 41: 3845–3858
- Farg MA, Sundaramoorthy V, Sultana JM, Yang S, Atkinson RA, Levina V, Halloran MA, Gleeson PA, Blair IP, Soo KY *et al* (2014) C9ORF72, implicated in amyotrophic lateral sclerosis and frontotemporal dementia, regulates endosomal trafficking. *Hum Mol Genet* 23: 3579–3595
- Fratta P, Mizielska S, Nicoll AJ, Zloh M, Fisher EM, Parkinson G, Isaacs AM (2012) C9orf72 hexanucleotide repeat associated with amyotrophic lateral sclerosis and frontotemporal dementia forms RNA G-quadruplexes. *Sci Rep* 2: 1016
- Freibaum BD, Lu Y, Lopez-Gonzalez R, Kim NC, Almeida S, Lee KH, Badders N, Valentine M, Miller BL, Wong PC *et al* (2015) GGGGCC repeat expansion in C9orf72 compromises nucleocytoplasmic transport. *Nature* 525: 129–133
- Gendron TF, Bieniek KF, Zhang YJ, Jansen-West K, Ash PE, Caulfield T, Daugherty L, Dunmore JH, Castanedes-Casey M, Chew J *et al* (2013) Antisense transcripts of the expanded C9ORF72 hexanucleotide repeat form nuclear RNA foci and undergo repeat-associated non-ATG translation in c9FTD/ALS. *Acta Neuropathol* 126: 829–844
- Gijssels I, Van Langenhove T, van der Zee J, Slegers K, Piltjens S, Kleinberger G, Janssens J, Bettens K, Van Cauwenbergh C, Pereson S *et al* (2012) A C9orf72 promoter repeat expansion in a Flanders-Belgian cohort with disorders of the frontotemporal lobar degeneration-amyotrophic lateral sclerosis spectrum: a gene identification study. *Lancet Neurol* 11: 54–65
- Graham AC, Davis SM, Andrusis ED (2009) Interdependent nucleocytoplasmic trafficking and interactions of Dis3 with Rrp6, the core exosome and importin- $\alpha$ 3. *Traffic* 10: 499–513
- Haeusler AR, Donnelly CJ, Periz G, Simko EA, Shaw PG, Kim MS, Maragakis NJ, Troncoso JC, Pandey A, Sattler R *et al* (2014) C9orf72 nucleotide repeat structures initiate molecular cascades of disease. *Nature* 507: 195–200
- Januszyk K, Liu Q, Lima CD (2011) Activities of human RRP6 and structure of the human RRP6 catalytic domain. *RNA* 17: 1566–1577
- Kilchert C, Wittmann S, Vasiljeva L (2016) The regulation and functions of the nuclear RNA exosome complex. *Nat Rev Mol Cell Biol* 17: 227–239
- Kwon I, Xiang S, Kato M, Wu L, Theodoropoulos P, Wang T, Kim J, Yun J, Xie Y, McKnight SL (2014) Poly-dipeptides encoded by the C9orf72 repeats bind nucleoli, impede RNA biogenesis, and kill cells. *Science* 345: 1139–1145
- Lee YB, Chen HJ, Peres JN, Gomez-Deza J, Attig J, Stalekar M, Troakes C, Nishimura AL, Scotter EL, Vance C *et al* (2013) Hexanucleotide repeats in ALS/FTD form length-dependent RNA foci, sequester RNA binding proteins, and are neurotoxic. *Cell Rep* 5: 1178–1186
- Lee KH, Zhang P, Kim HJ, Mitrea DM, Sarkar M, Freibaum BD, Cika J, Coughlin M, Messing J, Molliex A *et al* (2016) C9orf72 dipeptide repeats impair the assembly, dynamics, and function of membrane-less organelles. *Cell* 167: 774–788
- Lopez-Gonzalez R, Lu Y, Gendron TF, Karydas A, Tran H, Yang D, Petrucelli L, Miller BL, Almeida S, Gao FB (2016) Poly(GR) in C9ORF72-related ALS/FTD compromises mitochondrial function and increases oxidative stress and DNA damage in iPSC-derived motor neurons. *Neuron* 92: 383–391
- Mackenzie IR, Arzberger T, Kremmer E, Troost D, Lorenzl S, Mori K, Weng SM, Haass C, Kretschmar HA, Edbauer D *et al* (2013) Dipeptide repeat protein pathology in C9ORF72 mutation cases: clinico-pathological correlations. *Acta Neuropathol* 126: 859–879
- Makino DL, Baumgartner M, Conti E (2013) Crystal structure of an RNA-bound 11-subunit eukaryotic exosome complex. *Nature* 495: 70–75
- Malet H, Topf M, Clare DK, Ebert J, Bonneau F, Basquin J, Drazkowska K, Tomecki R, Dziembowski A, Conti E *et al* (2010) RNA channelling by the eukaryotic exosome. *EMBO Rep* 11: 936–942
- May S, Hornburg D, Schludi MH, Arzberger T, Rentzsch K, Schwenk BM, Grasser FA, Mori K, Kremmer E, Banzhaf-Strathmann J *et al* (2014) C9orf72 FTLD/ALS-associated Gly-Ala dipeptide repeat proteins cause neuronal toxicity and Unc119 sequestration. *Acta Neuropathol* 128: 485–503
- Mitchell P, Petfalski E, Shevchenko A, Mann M, Tollervey D (1997) The exosome: a conserved eukaryotic RNA processing complex containing multiple 3'→5' exoribonucleases. *Cell* 91: 457–466
- Mizielska S, Gronke S, Niccoli T, Ridler CE, Clayton EL, Devoy A, Moens T, Norona FE, Woollacott IO, Pietrzyk J *et al* (2014) C9orf72 repeat expansions cause neurodegeneration in *Drosophila* through arginine-rich proteins. *Science* 345: 1192–1194
- Mizielska S, Ridler CE, Balendra R, Thoeng A, Woodling NS, Grasser FA, Plagnol V, Lashley T, Partridge L, Isaacs AM (2017) Bidirectional nucleolar dysfunction in C9orf72 frontotemporal lobar degeneration. *Acta Neuropathol Commun* 5: 29
- Mori K, Arzberger T, Grasser FA, Gijssels I, May S, Rentzsch K, Weng SM, Schludi MH, van der Zee J, Cruts M *et al* (2013a) Bidirectional transcripts of the expanded C9orf72 hexanucleotide repeat are translated into aggregating dipeptide repeat proteins. *Acta Neuropathol* 126: 881–893
- Mori K, Lammich S, Mackenzie IR, Forne I, Zilow S, Kretschmar H, Edbauer D, Janssens J, Kleinberger G, Cruts M *et al* (2013b) hnRNP A3 binds to GGGGCC repeats and is a constituent of p62-positive/TDP43-negative inclusions in the hippocampus of patients with C9orf72 mutations. *Acta Neuropathol* 125: 413–423
- Mori K, Weng SM, Arzberger T, May S, Rentzsch K, Kremmer E, Schmid B, Kretschmar HA, Cruts M, Van Broeckhoven C *et al* (2013c) The C9orf72 GGGGCC repeat is translated into aggregating dipeptide-repeat proteins in FTLD/ALS. *Science* 339: 1335–1338
- Mori K, Nihei Y, Arzberger T, Zhou Q, Mackenzie IR, Hermann A, Hanisch F, German Consortium for Frontotemporal Lobar D, Bavarian Brain Banking

- A, Kamp F et al (2016) Reduced hnRNP3 increases C9orf72 repeat RNA levels and dipeptide-repeat protein deposition. *EMBO Rep* 17: 1314–1325
- Nihei Y, Mori K, Werner G, Arzberger T, Zhou Q, Khosravi B, Japtok J, Hermann A, Sommacal A, Weber M et al (2020) Poly-glycine-alanine exacerbates C9orf72 repeat expansion-mediated DNA damage via sequestration of phosphorylated ATM and loss of nuclear hnRNP3. *Acta Neuropathol* 139: 99–118
- Prudencio M, Gonzales PK, Cook CN, Gendron TF, Daugherty LM, Song Y, Ebbert MTW, van Blitterswijk M, Zhang YJ, Jansen-West K et al (2017) Repetitive element transcripts are elevated in the brain of C9orf72 ALS/FTLD patients. *Hum Mol Genet* 26: 3421–3431
- Reddy K, Zamiri B, Stanley SY, Macgregor RB Jr, Pearson CE (2013) The disease-associated r(GGGGCC)<sub>n</sub> repeat from the C9orf72 gene forms tract length-dependent uni- and multimolecular RNA G-quadruplex structures. *J Biol Chem* 288: 9860–9866
- Renton AE, Majounie E, Waite A, Simon-Sanchez J, Rollinson S, Gibbs JR, Schymick JC, Laaksovirta H, van Swieten JC, Myllykangas L et al (2011) A hexanucleotide repeat expansion in C9ORF72 is the cause of chromosome 9p21-linked ALS-FTD. *Neuron* 72: 257–268
- Sareen D, O'Rourke JG, Meera P, Muhammad AK, Grant S, Simpkinson M, Bell S, Carmona S, Ornelas L, Sahabian A et al (2013) Targeting RNA foci in iPSC-derived motor neurons from ALS patients with a C9ORF72 repeat expansion. *Sci Transl Med* 5: 208ra149
- Sellier C, Campanari ML, Julie Corbier C, Gaucherot A, Kolb-Cheynel I, Oulad-Abdelghani M, Ruffenach F, Page A, Ciura S, Kabashi E et al (2016) Loss of C9ORF72 impairs autophagy and synergizes with polyQ Ataxin-2 to induce motor neuron dysfunction and cell death. *EMBO J* 35: 1276–1297
- Shi Y, Lin S, Staats KA, Li Y, Chang WH, Hung ST, Hendricks E, Linares GR, Wang Y, Son EY et al (2018) Haploinsufficiency leads to neurodegeneration in C9ORF72 ALS/FTD human induced motor neurons. *Nat Med* 24: 313–325
- Tomecki R, Kristiansen MS, Lykke-Andersen S, Chlebowski A, Larsen KM, Szczesny RJ, Drazkowska K, Pastula A, Andersen JS, Stepien PP et al (2010) The human core exosome interacts with differentially localized processive RNases: hDIS3 and hDIS3L. *EMBO J* 29: 2342–2357
- Wan J, Yourshaw M, Mamsa H, Rudnik-Schoneborn S, Menezes MP, Hong JE, Leong DW, Senderek J, Salman MS, Chitayat D et al (2012) Mutations in the RNA exosome component gene EXOSC3 cause pontocerebellar hypoplasia and spinal motor neuron degeneration. *Nat Genet* 44: 704–708
- Wasmuth EV, Lima CD (2012) Exo- and endoribonucleolytic activities of yeast cytoplasmic and nuclear RNA exosomes are dependent on the noncatalytic core and central channel. *Mol Cell* 48: 133–144
- Wasmuth EV, Januszyk K, Lima CD (2014) Structure of an Rps6-RNA exosome complex bound to poly(A) RNA. *Nature* 511: 435–439
- Wasmuth EV, Lima CD (2017) The Rps6 C-terminal domain binds RNA and activates the nuclear RNA exosome. *Nucleic Acids Res* 45: 846–860
- Webster CP, Smith EF, Bauer CS, Moller A, Hautbergue GM, Ferraiuolo L, Myszczyńska MA, Higginbottom A, Walsh MJ, Whitworth AJ et al (2016) The C9orf72 protein interacts with Rab1a and the ULK1 complex to regulate initiation of autophagy. *EMBO J* 35: 1656–1676
- Wen X, Tan W, Westergard T, Krishnamurthy K, Markandaiah SS, Shi Y, Lin S, Shneider NA, Monaghan J, Pandey UB et al (2014) Antisense proline-arginine RAN dipeptides linked to C9ORF72-ALS/FTD form toxic nuclear aggregates that initiate *in vitro* and *in vivo* neuronal death. *Neuron* 84: 1213–1225
- Xu Z, Poidevin M, Li X, Li Y, Shu L, Nelson DL, Li H, Hales CM, Gearing M, Wingo TS et al (2013) Expanded GGGGCC repeat RNA associated with amyotrophic lateral sclerosis and frontotemporal dementia causes neurodegeneration. *Proc Natl Acad Sci USA* 110: 7778–7783
- Yang M, Liang C, Swaminathan K, Herrlinger S, Lai F, Shiekhhattar R, Chen JF (2016) A C9ORF72/SMCR8-containing complex regulates ULK1 and plays a dual role in autophagy. *Sci Adv* 2: e1601167
- Zhang K, Donnelly CJ, Haeusler AR, Grima JC, Machamer JB, Steinwald P, Daley EL, Miller SJ, Cunningham KM, Vidensky S et al (2015) The C9orf72 repeat expansion disrupts nucleocytoplasmic transport. *Nature* 525: 56–61
- Zhang YJ, Gendron TF, Grima JC, Sasaguri H, Jansen-West K, Xu YF, Katzman RB, Gass J, Murray ME, Shinohara M et al (2016) C9ORF72 poly(GA) aggregates sequester and impair HR23 and nucleocytoplasmic transport proteins. *Nat Neurosci* 19: 668–677
- Zhang K, Daigle JG, Cunningham KM, Coyne AN, Ruan K, Grima JC, Bowen KE, Wadhwa H, Yang P, Rigo F et al (2018a) Stress granule assembly disrupts nucleocytoplasmic transport. *Cell* 173: 958–971
- Zhang YJ, Gendron TF, Ebbert MTW, O'Raw AD, Yue M, Jansen-West K, Zhang X, Prudencio M, Chew J, Cook CN et al (2018b) Poly(GR) impairs protein translation and stress granule dynamics in C9orf72-associated frontotemporal dementia and amyotrophic lateral sclerosis. *Nat Med* 24: 1136–1142
- Zhou Q, Lehmer C, Michaelsen M, Mori K, Alterauge D, Baumjohann D, Schludi MH, Greiling J, Farny D, Flatley A et al (2017) Antibodies inhibit transmission and aggregation of C9orf72 poly-GA dipeptide repeat proteins. *EMBO Mol Med* 9: 687–702
- Zhu Q, Jiang J, Gendron TF, McAlonis-Downes M, Jiang L, Taylor A, Diaz Garcia S, Ghosh Dastidar S, Rodriguez MJ, King P et al (2020) Reduced C9ORF72 function exacerbates gain of toxicity from ALS/FTD-causing repeat expansion in C9orf72. *Nat Neurosci* 23: 615–624
- Zu T, Liu Y, Banez-Coronel M, Reid T, Pletnikova O, Lewis J, Miller TM, Harms MB, Falchook AE, Subramony SH et al (2013) RAN proteins and RNA foci from antisense transcripts in C9ORF72 ALS and frontotemporal dementia. *Proc Natl Acad Sci USA* 110: E4968–E4977



**License:** This is an open access article under the terms of the Creative Commons Attribution-NonCommercial-NoDeriv 4.0 License, which permits use and distribution in any medium, provided the original work is properly cited, the use is non-commercial and no modifications or adaptations are made.